Analytic calculation of the anomalous exponents in turbulence: Using the fusion rules to flush out a small parameter

Victor S. L'vov and Itamar Procaccia
Department of Chemical Physics, The Weizmann Institute of Science, Rehovot 76100, Israel
(Received 12 May 2000)

The main difficulty of statistical theories of fluid turbulence is the lack of an obvious small parameter. In this paper we show that the formerly established fusion rules can be employed to develop a theory in which Kolmogorov's statistics of 1941 (K41) acts as the zero order, or background statistics, and the anomalous corrections to the K41 scaling exponents ζ_n of the nth-order structure functions can be computed analytically. The crux of the method consists of renormalizing a four-point interaction amplitude on the basis of the fusion rules. This amplitude includes a small dimensionless parameter, which is shown to be of the order of the anomaly of ζ_2, $\delta_2=\zeta_2-2/3\approx 0.03$. Higher-order interaction amplitudes are shown to be even smaller. The corrections to K41 to $O(\delta_2)$ result from standard logarithmically divergent ladder diagrams in which the four-point interaction acts as a ''rung.'' The theory allows a calculation of the anomalous exponents ζ_n in powers of the small parameter δ_2. The n dependence of the scaling exponents ζ_n stems from pure combinatorics of the ladder diagrams. In this paper we calculate the exponents ζ_n up to $O(\delta_2^3)$. Previously derived bridge relations allow a calculation of the anomalous exponents of correlations of the dissipation field and of dynamical correlations in terms of the same parameter δ_2. The actual evaluation of the small parameter δ_2 from first principles requires additional developments that are outside the scope of this paper.

PACS number(s): 47.27.Gs, 47.27.Jv, 05.40.−a

I. INTRODUCTION

The aim of this paper is to build on previous work to achieve a controlled evaluation of the anomalous exponents that characterize various correlation and structure functions in isotropic, homogeneous, and stationary Navier-Stokes turbulence, and in particular the exponents ζ_n that characterize nth-order structure functions. The main result of this paper is that given a single experimental input (for example, the value of the anomalous exponent of the second-order structure function), the n dependence of all the other exponents that were reliably measured in experiments and simulations can be calculated analytically.

Decades of experimental and theoretical attention (see, for example, Refs. [1–7]) have been devoted to two types of simultaneous correlation functions; the first type includes the structure functions of velocity differences

$$S_n(\boldsymbol{R})=\langle|\boldsymbol{u}(\boldsymbol{r}+\boldsymbol{R})-\boldsymbol{u}(\boldsymbol{r})|^n\rangle, \tag{1}$$

where $\langle\cdots\rangle$ stands for a suitably defined ensemble average. A second type of correlations include gradients of the velocity field. An important example is the rate $\epsilon(\boldsymbol{r},t)$ at which energy is dissipated into heat due to viscous damping. This rate is roughly $\nu|\nabla\boldsymbol{u}(\boldsymbol{r},t)|^2$. An often-studied simultaneous correlation function of $\hat{\epsilon}(\boldsymbol{r},t)=\epsilon(\boldsymbol{r},t)-\overline{\epsilon}$ is

$$K_{\epsilon\epsilon}(\boldsymbol{R})=\langle\hat{\epsilon}(\boldsymbol{r}+\boldsymbol{R})\hat{\epsilon}(\boldsymbol{r})\rangle. \tag{2}$$

It has been hypothesized by Kolmogorov in 1941 (K41) and 1962 (K62) that statistical objects of this type exhibit power-law dependence on R [1,8]:

$$S_n(R)\propto R^{\zeta_n},\quad K_{\epsilon\epsilon}(R)\propto R^{-\mu}. \tag{3}$$

In addition, the K41 theory predicted the values of ζ_n to be $n/3$. Experimental measurements and computer simulations show that in some aspects K41 was remarkably close to the truth. The major aspect of its predictions, that the statistical quantities depend on the length scale R as power laws, is corroborated by experiments. On the other hand, the predicted exponents seem not to be exactly realized. The numerical values of ζ_n deviate progressively from $n/3$ when n increases [3–6]. K62 tried to improve on this prediction by taking into account the fluctuations in the rate of energy dissipation. On the basis of a phenomenological model, assuming the distributions function of energy dissipation to be lognormal, K62 reached the predictions

$$\zeta_n=\frac{n}{3}-\frac{\mu n(n-3)}{18}. \tag{4}$$

In addition to the fact that these predictions did not follow from fluid mechanical considerations, it was pointed out [7] that they violate basic inequalities that do not allow the exponents ζ_n to decrease, something that always happens with Eq. (4) with n large enough. The quest for computing the scaling exponents from the equations of fluid mechanics was long, arduous, and on the whole pretty unsuccessful.

In this paper we present an approach that is based on our own previous findings which culminates in the analytic calculation of exponents such as ζ_n and μ. At present the calculation is not completely from first principles. We need the input of *one* number from experiment, say $\delta_2\equiv\zeta_2-2/3$. Given this number we can calculate all the other exponents systematically with δ_2 being a small parameter that organizes our calculations. To first order in δ_2 we recapture Eq. (4). We will show that the result to $O(\delta_2)$ is *universal*, independent of the details of the calculations performed below. To second order we find the results

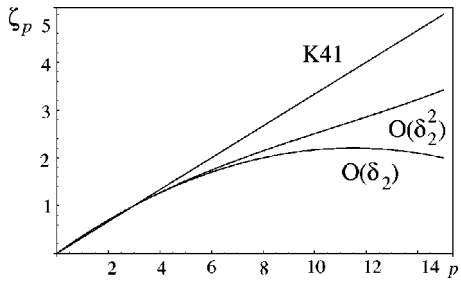

FIG. 1. The scaling exponents ζ_n as a function of n. The calculation is organized by the small parameter $\delta_2=\zeta_2-2/3\approx 0.03$. Shown is the K41 prediction which is zero order in δ_2, together with our results to first and second order in δ_2. To first order the results are the same as the phenomenological prediction of K62, and to second order it is Eq. (5) with $b_2=-0.55$ according to Eq. (72).

$$\zeta_n=\frac{n}{3}-\frac{n(n-3)}{2}\delta_2[1+2\delta_2(n-2)b_2]+O(\delta_2^3), \quad (5)$$

$$\mu=9\delta_2(1+8b_2\delta_2)+O(\delta_2^3). \quad (6)$$

The curves of ζ_n vs n are shown in Fig. 1, using the experimentally accepted value $\delta_2\approx 0.03$ [6]. We show the K41 prediction, the result of our calculation to one-loop order, and the two-loop result that is presented in Eq. (5). While the *form* of these results is universal, the numerical value of the dimensionless parameter b_2 depends on the details of the calculations; we find that b_2 is always negative and of the order of unity. Note that the two-loop results correct the unwanted down curving of the one-loop calculation (which is the same malaise as in K62).

In thinking about the strategy for this work we were led by some insights that developed in the context of understanding how to compute the scaling exponents of the Kraichnan model of passive scalar advection [9,10]. In that model a scalar field $T(\boldsymbol{r},t)$ is advected by a Gaussian velocity field $\boldsymbol{u}(\boldsymbol{r},t)$ which is δ-correlated in time but which has a scaling exponent $\zeta_2=\epsilon$. For $\epsilon=0$ the advected scalar has trivial statistics, and for ϵ small the model has a natural small parameter. It turned out that the calculation of the exponents can proceed along two lines. The first, which is nonperturbative, was pioneered in Ref. [11]. It considers the differential equations that the nth-order correlation functions satisfy, and identifies the anomalous scaling solutions as the zero modes of these differential equations. The calculation of the exponents then depends on the calculation of the zero modes themselves, a task that is not at all easy, and therefore such calculations were never done for any order but $O(\epsilon)$. In this method the renormalization scale is the outer scale L, not the inner scale η, and the dimensionless ratio of scales that carries the anomalous part of the exponents of the structure functions is L/R where R is defined in Eq. (1). A second method that was discussed in detail in Ref. [12] considers instead of the correlation functions the averages of higher moments of ∇T, i.e., $\langle|\nabla T|^n\rangle$. These quantities diverge as powers of L/η, and the exponents of this power are the same as the anomalous part of the exponent of the nth-order structure function. The great advantage of the second method is that one can write a perturbative theory in ϵ for the scaling exponents themselves, without any need to compute the zero modes or any other functions of many variables. Thus the second method allows computations to $O(\epsilon^2)$ [13,14] easily and with some more effort to higher orders. The insight gained is that one needs to focus on a quantity that offers the most feasible calculation, exposing the anomalous part of the exponents as it appears with a dimensionless ratio of length scales.

In Navier Stokes turbulence the situation is similar. On the one hand we have a nonperturbative theory which in this case is the infinite hierarchy formed by the equations of motion of the correlation function [15]. We can use this hierarchy to demonstrate that anomalous solutions exist, but the computation of the scaling exponents requires a calculation of the correlation functions themselves. This is a very difficult task that up to now has not been accomplished in a satisfactory manner. The other approach will be described in this paper. It will be a perturbative theory for the scaling exponents themselves, not requiring the computation of the correlation function along the way. Similarly to the second method in the Kraichnan problem it will be based on considering limits of correlation functions when p coordinates fuse. In that limit we create, even when all the distances are in the inertial range, a ratio of large and small lengthscales that appears raised to the power of the anomalous exponent ζ_n.

The two previous findings that influence the present formulation crucially are the mechanism for anomalous scaling that was announced in Ref. [16], and the fusion rules that were discussed in Ref. [17]. In short, Ref. [16] exposed ladder diagrams which appear in the theory of turbulence. These diagrams contain logarithmic divergences that are summable to power laws with anomalous exponents. These ladder diagrams contain ''rungs'' of the ladder, that are actually vertices with four, six, and more ''legs,'' representing four-point, six-point, and higher-order interaction amplitudes. In Ref. [16] these objects were represented in terms of infinite series of diagrams that could not be resummed analytically. This is where the fusion rules are now most useful. The fusion rules determine the asymptotic properties of n-point correlation functions when subgroups of p coordinates coalesce together. As such the fusion rules are nonperturbative, and are believed to be exact. We use the fusion rules to determine the asymptotic properties of the rungs. This is done such that a *calculation* of ζ_2 from the theory will agree with the experimental value of ζ_2. We then show that the knowledge of the asymptotics suffices for constructing a calculation of all the other scaling exponents, and in particular of ζ_n for $n>2$ and of μ. The crux is that in the process of determining the analytic form of the rungs we discover that their amplitude contains powers of a dimensionless small parameter $\delta_2=\zeta_2-2/3\approx 0.03$ [6]. Using this small parameter in the renormalized four-point interaction allows us to develop a systematic expansion in orders of δ_2. At the end of this paper we sketch a way to understand the remaining task regarding the origin of the small parameter $\zeta_2-2/3$.

One should stress at this point that fundamental differences exist with the Kraichnan problem. First, the second-order correlation function has exactly one diagram in its diagrammatic representation, and since the rung remains bare in the Kraichnan model, there is no way to dress the normal exponent. But once we go to higher-order objects the situa-

tion becomes very similar to the present Navier-Stokes case. Of course one cannot present in the Kraichnan case a solution for ζ_n in terms of ζ_2 or any lower order ζ_p—the problem is linear, decoupled, and therefore genuinely multiscaling. Our proposition is that in the case of Navier-Stokes the hierarchic coupling between various orders makes the problem less genuinely multiscaling.

In Sec. II we summarize past results that are necessary for the present developments. In Sec. III we show how the fusion rules can be used to determine the properties of the rungs in the ladder diagrams appearing in the nth-order correlation functions. The first important result is demonstrated in Sec. V—the numerical coefficient contained in the four-point rung is shown to be *small*, of the order of the anomaly of ζ_2. This result is crucial since it allows (to our knowledge for the first time) the development of a perturbative calculation of the anomalous parts of all the other exponents. The physical reason for this result is that (in Sec. IV) we are developing the theory around the K41 solution instead of the dissipative solution as was always attempted. In Sec. V we pave the way for the calculation of all the other exponents. In Sec. VI we calculate the scaling exponents by resumming the logarithmically divergent ladder diagrams up to $O(\delta_2)$ (which is known in field-theoretic jargon as the ''one-loop order'' in the renormalized rungs). We find (admittedly to our surprise) that to this order the scaling exponents are identical to K62. Similar to the latter they suffer from the violation of the known requirement that ζ_n cannot decrease with n [7]. In Sec. VII we show that the two-loop order solves the problem of K62, and we present the result (5) for ζ_n that in our theoretical estimate is valid for $n \leqslant 12$. The exponent μ is also computed in this section. If one wanted results for ζ_n with higher values of n one would need to go to three-loop order (and see Sec. VIII where the form of ζ_n to this order is presented), but the current experimental situation does not warrant a theoretical prediction of ζ_n for very high values of n. In Sec. VIII we summarize the paper, paying special attention to the range of validity of the theory and to demonstrating that no uncontrolled approximations were made.

II. SUMMARY OF PERTINENT PREVIOUS RESULTS

In this section we present a brief summary of some past work which is most pertinent. We refer to Ref. [19] as paper I, to Ref. [16] as paper II, and to Ref. [18] as paper III.

A. The basic perturbation theory

The starting point of the analysis are the Navier-Stokes equations for the velocity field of an incompressible fluid with kinematic viscosity ν which is forced by an external force $\boldsymbol{f}(\boldsymbol{r},t)$:

$$\left(\frac{\partial}{\partial t}-\nu\Delta^2\right)\boldsymbol{u}+\vec{\boldsymbol{P}}(\boldsymbol{u}\cdot\boldsymbol{\nabla})\boldsymbol{u}=\vec{\boldsymbol{P}}\boldsymbol{f}, \tag{7}$$

where $\vec{\boldsymbol{P}}$ is the transverse projection operator $\vec{\boldsymbol{P}}\equiv-\Delta^{-2}\boldsymbol{\nabla}\times\boldsymbol{\nabla}\times$. It is well known (see, for example, paper I) that developing a perturbative approach [20–22] for the correlation functions and response functions in terms of the Eulerian velocity $\boldsymbol{u}(\boldsymbol{r},t)$ results in a theory that is plagued with infrared divergences. On the other hand, one can transform to new variables, and after the transformation (which amounts to infinite partial resummations in the perturbation theory) one finds a renormalized perturbation theory that is finite, without any divergences in any order of the expansion (see Ref. [23] and paper I) . One can achieve such a theory using Lagrangian variables [24]; we find it technically simpler to employ the Belinicher-L'vov transformation [23]

$$\boldsymbol{v}[\boldsymbol{r}_0|\boldsymbol{r},t]\equiv\boldsymbol{u}[\boldsymbol{r}+\boldsymbol{\rho}(\boldsymbol{r}_0,t),t], \tag{8}$$

where $\boldsymbol{\rho}(\boldsymbol{r}_0,t)$ is the Lagrangian trajectory of a fluid point which has started at point $\boldsymbol{r}=\boldsymbol{r}_0$ at time $t=t_0$

$$\boldsymbol{\rho}(\boldsymbol{r}_0,t)=\int_0^t\boldsymbol{u}[\boldsymbol{r}+\boldsymbol{\rho}(\boldsymbol{r}_0,\tau),\tau]d\tau. \tag{9}$$

The natural variables for a divergence free theory are the velocity *differences*

$$\boldsymbol{w}(\boldsymbol{r}_0|\boldsymbol{r},t)\equiv\boldsymbol{v}[\boldsymbol{r}_0|\boldsymbol{r},t]-\boldsymbol{v}[\boldsymbol{r}_0|\boldsymbol{r}_0,t]. \tag{10}$$

Since the averages of quantities that depend on one time only can be computed at $t=0$, it follows that the average moments of these BL variables are the structure functions of the Eulerian field $S_n(\boldsymbol{R})$ defined by Eq. (1). It was shown [23] that these variables satisfy the Navier Stokes equations, and that one can develop (see paper I) a perturbation theory of the diagrammatic type in which the natural quantities are the Green's function $G_{1,1}^{\alpha\beta}(\boldsymbol{r}_0|\boldsymbol{r},\boldsymbol{r}',t,t')$ and the correlation function $F_2^{\alpha\beta}(\boldsymbol{r}_0|\boldsymbol{r},\boldsymbol{r}',t,t')$:

$$G_{1,1}^{\alpha\beta}(\boldsymbol{r}_0|\boldsymbol{r},\boldsymbol{r}',t,t')=\left\langle\frac{\delta w_\alpha(\boldsymbol{r}_0|\boldsymbol{r},t)}{\delta f_\beta(\boldsymbol{r}',t')}\right\rangle\Bigg|_{f\to0}, \tag{11}$$

$$F_2^{\alpha\beta}(\boldsymbol{r}_0|\boldsymbol{r},\boldsymbol{r}',t,t')=\langle w_\alpha(\boldsymbol{r}_0|\boldsymbol{r},t)w_\beta(\boldsymbol{r}_0|\boldsymbol{r}',t')\rangle. \tag{12}$$

Physically the Green's function is the mean response of the velocity difference to the action of a vanishingly small forcing. In stationary turbulence these quantities depend on $t'-t$ only, and we can denote this time difference as t. The quantities satisfy the well-known and exact Dyson and Wyld coupled equations. The Dyson equation reads

$$\begin{aligned}\left[\frac{\partial}{\partial t}-\nu\Delta\right]&G_{1,1}^{\alpha\beta}(\boldsymbol{r}_0|\boldsymbol{r},\boldsymbol{r}',t)\\&=G_{1,1}^{0;\alpha\beta}(\boldsymbol{r}_0|\boldsymbol{r},\boldsymbol{r}',0^+)\,\delta(t)+\int d\boldsymbol{r}_2G_{1,1}^{0;\alpha\delta}(\boldsymbol{r}_0|\boldsymbol{r},\boldsymbol{r}_2,0^+)\\&\quad\times\int d\boldsymbol{r}_1\int_0^t dt_1\Sigma_{\delta\gamma}(\boldsymbol{r}_0|\boldsymbol{r}_2,\boldsymbol{r}_1,t_1)G_{1,1}^{\gamma\beta}(\boldsymbol{r}_0|\boldsymbol{r}_1,\boldsymbol{r}',t-t_1),\end{aligned} \tag{13}$$

where $G_{1,1}^{0;\alpha\beta}(\boldsymbol{r}_0|\boldsymbol{r},\boldsymbol{r}',0^+)$ is the bare Green's function determined by Eq. (3.20) in paper I. The Wyld equation has the form

$$F_2^{\alpha\beta}(\boldsymbol{r}_0|\boldsymbol{r},\boldsymbol{r}',t)=\int d\boldsymbol{r}_1 d\boldsymbol{r}_2 \int_0^\infty dt_1 dt_2 G_{1,1}^{\alpha\gamma}(\boldsymbol{r}_0|\boldsymbol{r},\boldsymbol{r}_1,t_1) \times[D_{\gamma\delta}(\boldsymbol{r}_1-\boldsymbol{r}_2,t-t_1+t_2) + \Phi_{\gamma\delta}(\boldsymbol{r}_0|\boldsymbol{r}_1,\boldsymbol{r}_2,t-t_1+t_2)] \times G_{1,1}^{\delta\beta}(\boldsymbol{r}_0|\boldsymbol{r}',\boldsymbol{r}_2,t_2). \quad (14)$$

In Eq. (13) the ''mass operator'' Σ is related to the ''eddy viscosity'' whereas in Eq. (14) the ''mass operator'' Φ is the renormalized ''nonlinear'' noise which arises due to turbulent excitations. Both these quantities are dependent on the Green's function and the correlator, and thus the equations are coupled.

The main result of Paper I is a demonstration of the property of ''locality'' in the Dyson and Wyld equations. This property means that given a value of $|\boldsymbol{r}-\boldsymbol{r}_0|$ in Eq. (13), the important contribution to the integral on the right-hand side (RHS) comes from that region where $|\boldsymbol{r}_1-\boldsymbol{r}_0|$ and $|\boldsymbol{r}_2-\boldsymbol{r}_0|$ are of the order of $|\boldsymbol{r}-\boldsymbol{r}_0|$. In other words, all the integrals converge both in the upper and the lower limits. The same is true for the Wyld equation, meaning that in the limit of large L and small η these length scales disappear from the theory, and there is no natural cutoff in the integrals in the perturbative theory. In this case one cannot form a dimensionless parameter such as L/r or r/η to carry dimensionless corrections to the K41 scaling exponents. For $\eta \ll |\boldsymbol{r}-\boldsymbol{r}_0| \ll L$ scale invariance prevails, and one finds precisely the K41 scaling exponents

$$G_{1,1}^{\alpha\beta}(\lambda\boldsymbol{r}_0|\lambda\boldsymbol{r},\lambda\boldsymbol{r}',\lambda^z t)=\lambda^{\beta_2} G_{1,1}^{\alpha\beta}(\boldsymbol{r}_0|\boldsymbol{r},\boldsymbol{r}',t), \quad (15)$$

$$F_2^{\alpha\beta}(\lambda\boldsymbol{r}_0|\lambda\boldsymbol{r},\lambda\boldsymbol{r}',\lambda^z t)=\lambda^{\zeta_2} F_2^{\alpha\beta}(\boldsymbol{r}_0|\boldsymbol{r},\boldsymbol{r}',t).$$

One can derive two scaling relations which hold order-by-order, i.e.,

$$2z+\zeta_2=2, \quad z+2\zeta_2=2. \quad (16)$$

The solution is $z=\zeta_2=2/3$. It was also shown that the scaling exponent of the Green's function (15) is $\beta_2=-3$. Extending such considerations to the higher order structure functions leads to the order-by order K41 prediction that $\zeta_n = n/3$.

Of course, the order-by-order result (15) which leads to Eq. (16) is not necessarily the correct one. If one could resum all the diagrammatic expansion one could find nonperturbative answers that may be different. The whole sum of diagrams may diverge when the outer scale goes to infinity or the inner scale to zero, allowing a renormalization scale to creep in even though the order-by-order theory is convergent. Indeed, this mechanism was demonstrated explicitly in the case of the Kraichnan model [25]. The infinite series for the correlation functions F_n are convergent order-by-order as in the the Navier-Stokes case. In this case the perturbation expansions were resummed analytically, yielding equations for F_n (that were the same as the equations that were originally derived by Kraichnan [9]). These equations have forced solutions which are identical to the initial order-by-order expansion, but in addition they have zero modes of nonperturbative nature, which diverge when the outer scale goes to infinity. The conclusion is that indeed the infinite series for F_n hides a divergence that could be exposed by an exact resummation. The difficulty with the Navier-Stokes case is that no one knows how to resum the infinite expansion which exhibits no obvious small parameter.

In this paper we will propose a way out of this difficulty. It is based on the fusion rules. Instead of considering fully unfused correlation functions only, we will allow some coordinates to be much closer together, say within a distance $\boldsymbol{r}$, whereas the rest will be separated by a much larger distance, say of the order of $\boldsymbol{R}$ where $r \ll R$. We will show that we can form a dimensionless ratio with R/r and that such ratios carry anomalous exponents that are going to survive the process of fusion of coordinates in correlation functions when we make structure functions. We will thus be able to recognize the anomalous exponents even though at first sight there is no obvious renormalization scale.

To clarify how this mechanism works we need to remind ourselves how ladder diagrams appear in the theory of correlations functions. Such diagrams appear in the most transparent way in nonlinear Green's functions, and we review briefly our past results on these objects.

B. The nonlinear Green's functions

The nonlinear Green's function $G_{2,2}(\boldsymbol{r}_0|x_1,x_2,x_3,x_4)$ describes the mean value of the product of two responses of the velocity differences taken at different space-time coordinates to the action of the force $\boldsymbol{f}$:

$$G_{2,2}^{\alpha\beta\gamma\delta}(\boldsymbol{r}_0|x_1,x_2,x_3,x_4)=\left\langle \frac{\delta w_\alpha(\boldsymbol{r}_0|x_1)}{\delta f_\beta(\boldsymbol{r}_0|x_3)} \frac{\delta w_\gamma(\boldsymbol{r}_0|x_2)}{\delta f_\delta(\boldsymbol{r}_0|x_4)} \right\rangle_{f\to 0}, \quad (17)$$

where for brevity we use the notation $x_j \equiv \{\boldsymbol{r}_j,t_j\}$. Similarly, one defines the nonlinear Green's functions $\boldsymbol{G}_{n,n}$ as the mean value of the product of n such responses taken at distinct points to the action of n forces in different points. In particular the linear Green's function (11) corresponds to $n=1$.

In a Gaussian theory (which ours is not) $\boldsymbol{G}_{2,2}$ would be the products of two linear Green's functions such as $G_{1,1}{}^{\alpha\beta}(\boldsymbol{r}_0|x_1,x_3)G_{1,1}{}^{\gamma\delta}(\boldsymbol{r}_0|x_2,x_4)$. In a non-Gaussian theory one could assume that this quantity is a homogeneous function of its arguments when they are in the scaling regime. This means that

$$G_{2,2}^{\alpha\beta\gamma\delta}(\boldsymbol{r}_0|\lambda\boldsymbol{r}_1,\lambda^z t_1,\lambda\boldsymbol{r}_2,\lambda^z t_2,\lambda\boldsymbol{r}_3,\lambda^z t_3,\lambda\boldsymbol{r}_4,\lambda^z t_4) = \lambda^{\beta_4} G_{2,2}^{\alpha\beta\gamma\delta}(\boldsymbol{r}_0|x_1,x_2,x_3,x_4). \quad (18)$$

From the Gaussian decomposition of this quantity we would guess that $\beta_4=2\beta_2=-6$. We know by now that the assumption of homogeneity (18) is wrong for different-time objects [26]. Notwithstanding, the proof of locality in paper II means that there is no way from an order-by order approach to change the scaling index that follows from the homogeneity assumption. On the other hand, this quantity, which is a function of four space-time coordinates x_i has scaling properties that are not exhausted by the overall scaling exponent β_4. In thinking about such objects one needs to remember that in turbulence one forces the velocity field at

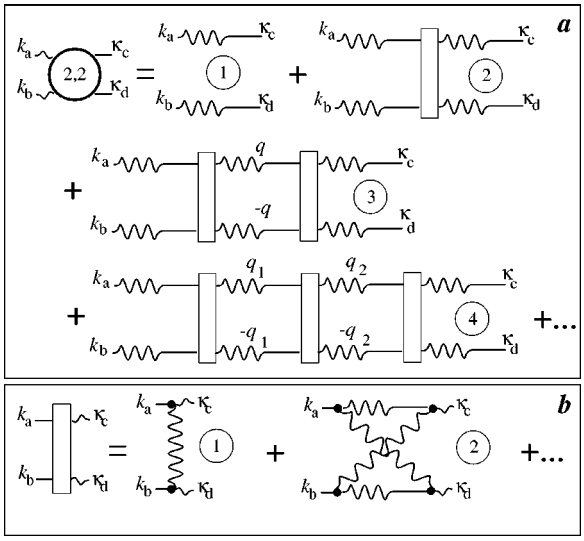

FIG. 2. Diagrams for $\mathbf{G}_{2,2}(\mathbf{k}_a,\omega_a,\mathbf{k}_b,\omega_b,\boldsymbol{\kappa}_c,\omega_c,\boldsymbol{\kappa}_d,\omega_d)$ (a) and of the rung $\mathbf{R}(\mathbf{k}_a,\mathbf{k}_b,\boldsymbol{\kappa}_c,\boldsymbol{\kappa}_d)$ (b). Diagram (1) in (a) is the Gaussian contribution made of a product of two linear Green's functions. Diagram (2) is the skeleton contribution, and diagrams (3) and (4) are the one-loop and two-loop contributions respectively. In (b) we show the beginning of the infinite series expansion for the rung, with diagram (1) being the bare rung.

the boundaries (with forces of characteristic scale L), and measures correlation functions at the interior. Universal scaling exponents are expected when all the distances $|\boldsymbol{r}_i-\boldsymbol{r}_j|, 1\leqslant i,j\leqslant n$ are of the order of $r\ll L$. In this sense these correlation functions are actually response functions. It should not come as a surprise then that the same scaling exponents are also exhibited by the genuine nth-order response functions $G_{n,n}$ which are the average response of n velocity differences to n forces. For example, when we think about $G_{2,2}$ we should expect that when $|\boldsymbol{r}_1-\boldsymbol{r}_2|\to r$ and r is much smaller than all the other five distances involved here, $\boldsymbol{G}_{2,2}$ scales as r^{ζ_2} and in general in the corresponding limit $G_{n,n}$ scales as r^{ζ_n} (a further discussion of the fusion limit is offered in Sec. III). It is thus natural to consider these nonlinear Green's function if one wants to evaluate the scaling exponents.

The physics of response functions in hydrodynamics is the following. There is always an uncorrelated response at the points of observation to the far away forcing. Thus $\boldsymbol{G}_{2,2}$ always has ''Gaussian'' contributions of the form $G_{1,1}(\boldsymbol{r}_1,t_1,\boldsymbol{r}_3,t_3)G_{1,1}(\boldsymbol{r}_2,t_2,\boldsymbol{r}_4,t_4)$. This contribution is shown as a pair of half wavy and half straight lines in Fig. 2. (In the figure $\boldsymbol{G}_{2,2}$ is denoted in $\boldsymbol{k},\omega$ representation.) In addition, there are contributions that arise due to hydrodynamic processes. The forcings at $\boldsymbol{r}_3,t_3$ and $\boldsymbol{r}_4,t_4$ give rise to intermediate responses at intermediate pairs of space-time points, affecting later responses at the points of observations $\boldsymbol{r}_1,t_1$ and $\boldsymbol{r}_2,t_2$. Such contributions are shown as the skeleton diagram in Fig. 2. The totality of such intermediate processes is represented by the rectangle, and of course one needs to integrate over all intermediate spatial positions and times. In addition, there are responses that are mitigated by more intermediate space-time points, and these are shown as the one-loop and two-loop diagrams in Fig. 2. The total response function is evidently the sum of all these contributions, taking into account all the possible intermediate hydrodynamic interactions giving rise to the response to far away forcing. We thus are able to represent the response function $G_{2,2}$ in terms of integrals in which the integrands are consists of a number of the standard Green's function and a new four-point interaction amplitude. On the one hand we have no idea at this point what this four-point object is. But on the other hand we have eliminated from the problem the three-point standard hydrodynamic vertex $(\boldsymbol{u}\boldsymbol{\nabla})\boldsymbol{u}$. This is not a minor feat, since this vertex is protected by Galilean invariance. No renormalization can make it in ''small'' anyway, and this has been one of the central difficulties of the theory of turbulence for a long time. The elimination of the *explicit* participation of the three-point vertex from the theory of anomalous scaling opens a possibility of having a small parameter in the higher-order interaction amplitudes. Indeed, we will show momentarily that this is the case: the four-point vertex is *small*, giving us a way to present a systematic theory with a small parameter.

If the reader is puzzled by the physical arguments presented here, we should stress that the diagrammatic expansion of Fig. 2 had been formally derived from standard perturbation theory in paper II. The simple ladder diagrams shown here are *all the terms* that appear in $\boldsymbol{G}_{2,2}$ as defined in Eq. (17). There are other contributions with different topologies that appear in similar quantities such as $\langle w_1\delta^2 w_2/\delta f_3\delta f_4\rangle$, but for the average product of two responses Fig. 2(a) is *everything*. It is easy to understand why this is so: when we consider the average of a *product* of two responses, each response must contain one line of Green's function connecting the point of response to the point of forcing, with the orientation of the Green's function as shown in Fig. 2(a). When we form the product, we must have two ''struts'' to the ladder such that the Green's function appear in pairs with the same orientation. Other 2-2 responses can contain inverted Green's functions or correlators instead of Green's function, but this is not possible for $\boldsymbol{G}_{2,2}$ as defined in Eq. (17).

In paper II the four-point rungs were presented in terms of an infinite series whose beginning is shown in Fig. 2(b). In terms of the physical explanation given above it is not surprising that the first contribution is a two-point correlation function with two standard three-point vertices—this is precisely the origin of the correlated response that was discussed above. In addition we have shown in paper II that when we consider the dependence of $\boldsymbol{G}_{2,2}$ on *ratios* of space-time coordinates in their asymptotic regimes we pick up a set of anomalous scaling exponents. The main result of paper II was that in the regime $r_1\sim r_2\ll r_3\sim r_4$ the diagrammatic expansion of this object produces logarithms such as $\ln(r_3/r_1)$ to some power. It was explained that the sum of such logarithmically large contributions is given by $(r_3/r_1)^{\Delta}$ with some anomalous exponent Δ. Just from general properties one could show that the ladder with n rungs contains a contribution which is exactly $[\Delta\ln(r_3/r_1)]^n/n!$. The summation of all these contributions gives a term proportional to $(r_3/r_1)^{\Delta}$, and this is the observation that we want to build on in this paper. In later sections we will return to this mechanism of logarithmic divergence and the ladder resummation to anomalous exponents in full detail, but at this point we need to explain the connection of the observation to the fusion rules.

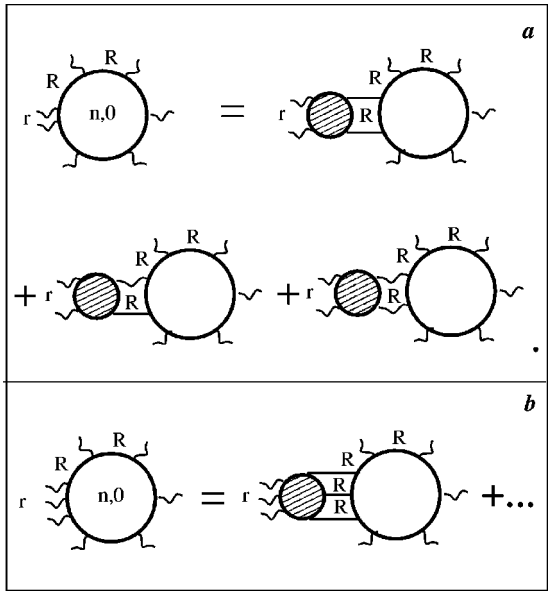

FIG. 3. A diagrammatic representation of the fusion process. A typical nth-order correlation function is represented by n wavy lines decorating a circle. (a) The fusion of two coordinates to within a distance r which is much smaller than the typical separations R between the other coordinates. All the existing diagrams are shown. (b) The fusion of three coordinates to within a distance $r \ll R$ from each other. In this case we show only the diagram with $G_{3,3}$ as the fragment carrying the scaling exponent ζ_3.

III. FUSION RULES AND LADDER DIAGRAMS IN HIGHER-ORDER CORRELATION FUNCTIONS

In this section we demonstrate how the anomalous exponents of the correlation functions can be related to resummed ladder diagrams. The idea is to consider a typical nth-order correlation function and to almost fuse p coordinates, $p<n$, chosen from the available n coordinates. The point to observe is that the diagrammatic theory allows us to write, upon observation, all the topologically possible diagrams appearing in the expansion of a given object. Thus, for example, consider Fig. 3 where we represent a general nth-order correlation function, in which two coordinates are a distance r from each other, and all the rest are a distance R from them and from each other. While coalescing the two coordinates we pull out all the possible diagrammatic fragments that are allowed by the topological rules, connecting the two fusing coordinates with the body of the diagram for the nth-order correlation functions. To the reader who is less familiar with diagrammatic representation we comment that these fragments represent the totality (the sum of) all the diagrams that have less than three legs at their end, before entering the body of the nth-order correlation function which by necessity must have more legs. The fragments pulled out can connect to the body either with two straight lines, or one straight and one wavy, or two wavy lines. The last is nothing but the fourth-order correlation function, whereas the first two are the *full* response functions of two velocities to two forcings, and three velocities to one forcing. The latter is known as $\boldsymbol{G}_{3,1}$. We should stress that the full response of two velocities to two forcings contains one contribution that is precisely $\boldsymbol{G}_{2,2}$ of Eq. (17). In addition it contains two additional 2-2 responses such as $\langle w_1 \delta^2 w_2 / \delta f_3 \delta f_4 \rangle$, etc. These additional objects are also represented diagrammatically as series of ladder diagrams, but their topology differs from $\boldsymbol{G}_{2,2}$ of Eq. (17), with four-point rungs of different types.

We are interested in the fusion limit in which $r \ll R$. Due to the property of diagrams called ''rigidity'' in paper III one can show that the dominant contribution to the diagrams in Fig. 3 comes from the region of integration in which the separation between the two last legs of fragments (connecting to the body) is of the order of R. Accordingly, we can analyze the r dependence of each of the fragments using the fusion rules when $r \ll R$ separately for the fragments themselves. Very importantly, all these contributions have the same leading exponent in r, which is ζ_2, in the fusing limit $r \ll R$. This result follows from the fusion rules [17]. For the fragment F_4 this is almost obvious; fusing two coordinates in a fourth-order correlation function results in r^{ζ_2} scaling. For the Green's functions one needs to convince oneself that it follows as well. The way to do it is to write the Green's functions as sums and differences of two-point correlation functions of velocity differences at different values of the forcing—each contribution will scale as r^{ζ_2}—multiplied by some function that depends on the large scales. These different prefactor functions cannot possibly cancel the leading order scaling result. This natural conclusion can be supported by the full diagrammatic theory of paper III in which it is shown that the exact equations for $\boldsymbol{G}_{2,2}$, $\boldsymbol{G}_{3,1}$, and $\boldsymbol{F}_4$ are all coupled together, giving rise to the same asymptotic exponent for all these objects in the fusion limit.

Accordingly, if we want to calculate the anomalous contribution to ζ_2 we can consider the ladder resummation of any of these contributions, and in particular of $\boldsymbol{G}_{2,2}$ of Eq. (17). Thus the anomaly of ζ_2 is represented by the sum of the ladder diagrams that we display in Fig. 2. We thus state that whenever we are about to fuse two coordinates in any nth-order correlation function we can expose a series of diagrams that are the same as those that appear in the expansion of the nonlinear Green's function $G_{2,2}(\boldsymbol{r}_0|x_1,x_2,x_3,x_4)$, together with the logarithmic divergences that are associated with them. In doing so we really take into account all the necessary contributions, leaving nothing uncontrolled.

Similarly, we can almost fuse 3, 4, or p coordinates, and accordingly pull out of the diagram for the nth-order correlation functions fragments that have 3, 4, or p wavy lines on the left, connected to the body of the diagrams with any number of wavy and straight lines such that this number sums up to 3, 4, or p, respectively. As before, we can argue that in the fusion limit all these fragments have the same exponent in r, r^{ζ_p}, when $r \ll R$. It is thus sufficient, for the consideration of say ζ_3, to consider the fragment shown in Fig. 2(b), and to focus on $G_{3,3}$ which is the average of the product of three responses. This quantity has the relatively simple ladder expansion which is shown explicitly in Fig. 4. In a similar way to $\boldsymbol{G}_{3,3}$ whose ladder diagrams have three struts, $\boldsymbol{G}_{p,p}$ will have ladder with p struts made of Greens' function $\boldsymbol{G}_{1,1}$ oriented from left to right. The fusion rules guarantee that the nth-order correlation is a homogeneous function of the p fusing coordinates with ζ_p being the homogeneity exponent. We will show that these more complex ladders also resum into power laws in R/r, being responsible for the anomalous parts of ζ_p.

At this point all this is a bit formal, since we do not have

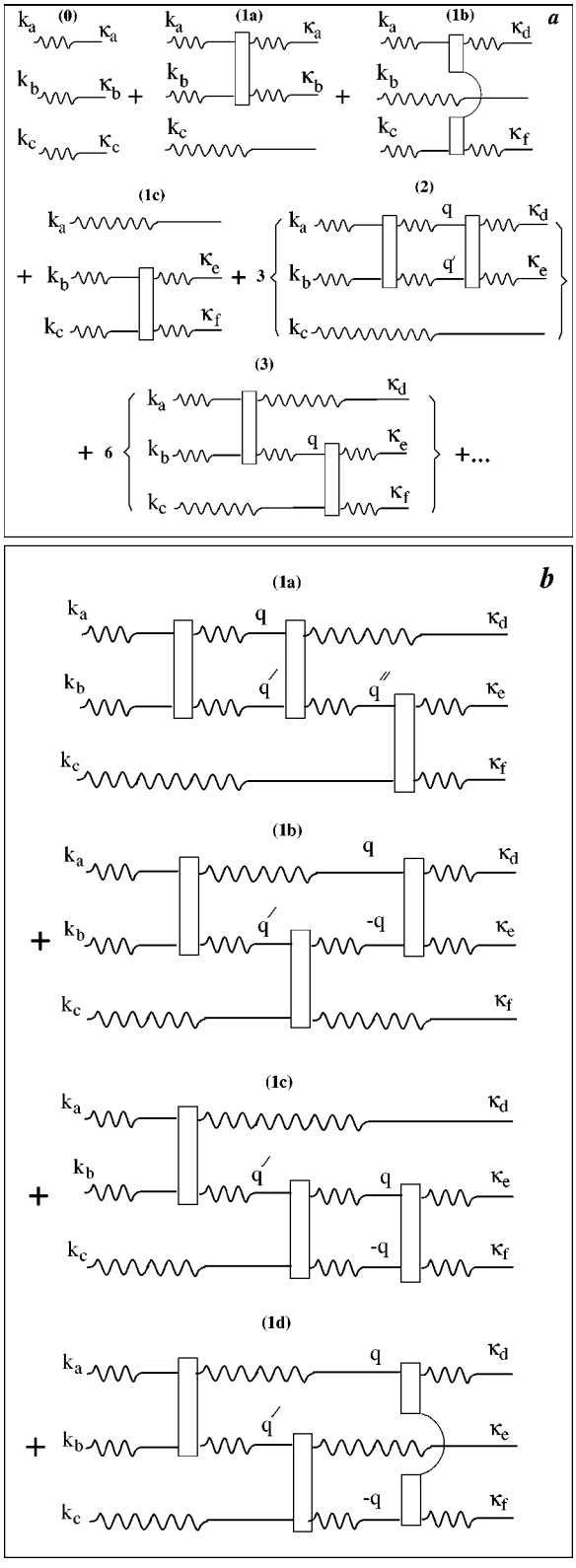

FIG. 4. Diagrammatic expansion of $\mathbf{G}_{3,3}$ (a) Contributions with no rungs, (diagram 0), one rung and two rungs. (b) Contributions with three rungs.

an explicit form of the rungs in the ladder diagrams, and we can compute nothing without this knowledge. In the next two sections we will address this issue and demonstrate that a judicious use of the fusion rules dictates enough knowledge of the rungs to take us through a useful calculation.

IV. BUILDING THE THEORY ON THE BACKGROUND OF K41

In this section we reorganize the theory such that Kolmogorov's 41 theory serves as its ''free'' limit. In other words, we aim at achieving a theory in which resummations of divergent contributions would directly give the *anomalous* parts of the scaling exponents; the K41 parts should be obvious order-by-order. This is done in two steps, that are correspondingly presented in Secs. IV A and IV B.

A. Resummation into K41 propagators

It was explained in Sec. II A that our theory is developed in the BL representation, to eliminate spurious IR divergences that stem from the sweeping interactions. The main result of paper I was that after line resummation each diagram in the BL-diagrammatic expansion of the propagators (Green's function and double correlation function) converged in the infrared and the ultraviolet regimes. Accordingly, K41 scaling is a solution of the order-by-order theory. Nevertheless, the propagators in the BL representation lose translational invariance, and are therefore not diagonal in Fourier space. For the purpose of actual calculations it is extremely advantageous to rearrange the theory such that the BL propagators become again diagonal in Fourier space.

The actual resummation that is necessary is presented in Appendix A. It results in a diagrammatic theory that is topologically exactly the same as the standard Wyld diagrammatic expansion before line resummation. There are two differences as explained in Appendix A. For the purposes of our considerations below the main issue is the simple form of the the propagators that appear as lines in the diagrams: they exhibit K41 scaling exponents

$$G_{1,1}^{\alpha\beta}(\boldsymbol{k},\omega)=P_{\alpha\beta}(\boldsymbol{k})g(k,\omega),\quad g(k,\omega)=\frac{1}{\omega+i\gamma(k)}, \tag{19}$$

$$F_{2}^{\alpha\beta}(\boldsymbol{k},\omega)=P_{\alpha\beta}(\boldsymbol{k})f(k,\omega),\quad f(k,\omega)=\frac{\phi(k)}{\omega^2+\gamma^2(k)}. \tag{20}$$

In these formulas the scaling exponents are carried by

$$\gamma(k)=c_\gamma\overline{\epsilon}^{1/3}k^{2/3},\quad \phi(k)=c_\phi\overline{\epsilon}k^{-3}, \tag{21}$$

where c_γ and c_ϕ are dimensionless constants.

B. Renormalization to K41 four-point rung

In this section we determine the form of the four-point rungs of the ladder diagrams in two steps. These two steps are based on the following observation: the diagrammatic expansion of the rung includes many diagrams, some of which contain in them additional subsets of ladder diagrams. In the first step we will consider the rungs as if all the diagrams appearing in their infinite series were resummed, *except* for their own internal subsets of ladder diagrams. In the second step we will consider also the ladder diagrams appearing in the series for the rung. We aim for a situation in which all the ladders that appear in the theory, as in Fig. 2,

already contain renormalized rungs. However, instead of evaluating the rungs from actual resummations we are going to determine their form using the fusion rules. Thus in the first step we find the form of the rung that results, upon fusion, in K41 scaling exponents. In the second step we recognize that the rungs themselves have ladders, leading to an anomalous correction in the scaling properties of the rungs themselves. This being accomplished, we will have our final form of the rung. Then we turn to the ladder diagrams appearing in the fused correlation functions, using the rung as a basic building block of the theory. All anomalies of all the measurable statistical objects will result from resummations of the remaining ladder diagrams.

Consider Fig. 2(a), in which the rung appears as an object. It is given in terms of an infinite series of diagrams in Fig. 2(b). It is in fact a four-point vertex depending on four $\boldsymbol{k}$ vectors and four frequencies. As a first step we consider the value of the rung when all the frequencies are zero, denoting it in this limit as $\boldsymbol{R}(\boldsymbol{k}_a,\boldsymbol{k}_b,\boldsymbol{\kappa}_c,\boldsymbol{\kappa}_d)$. At a later point we will explain that this is sufficient for our purposes. The bare value of this object can be read directly from diagram (1) in Fig. 2(b), with two bare BL vertices $\boldsymbol{\Gamma}$ and one double correlation function. The answer is

$$R_0^{\alpha\beta\gamma\delta}(\boldsymbol{k}_a,\boldsymbol{k}_b,\boldsymbol{\kappa}_c,\boldsymbol{\kappa}_d) = \delta_0\overline{\epsilon}^{1/3}\frac{\Gamma^{\alpha\gamma\sigma}(\boldsymbol{k}_a,\boldsymbol{\kappa}_c,\boldsymbol{k}_e)\Gamma^{\beta\delta\sigma}(\boldsymbol{k}_b,\boldsymbol{\kappa}_d,-\boldsymbol{k}_e)}{k_e^{13/3}}, \tag{22}$$

where $\boldsymbol{k}_e\equiv\boldsymbol{k}_a-\boldsymbol{\kappa}_c=\boldsymbol{\kappa}_d-\boldsymbol{k}_b$, and δ_0 is a dimensionless constant.

We demonstrate now that if we use this bare form of the rung the fusion rules would predict *dissipative* exponents $\zeta_n=n$. We first demonstrate this in the context of ζ_2. Consider a general nth-order correlation function and fuse two coordinates, pulling out the fragment of $\boldsymbol{G}_{2,2}$ as explained in the beginning of Sec. III. We will now compute the scaling exponent by finding the r dependence of this fragment when the two coordinates approach each other to a *small* distance $r\ll R$ where R is the typical distance between all the other coordinates. To find the r dependence we must integrate according to the explanation in Appendix B, and to this aim we introduce the object $T_2(r,\boldsymbol{\kappa})$ (which is ''longitudinal'' in the sense defined in Appendix B):

$$T_2(r,\boldsymbol{\kappa})=\int\frac{d\boldsymbol{k}_a}{(2\pi)^3}\,4\sin^2\!\left(\frac{1}{2}\,\boldsymbol{k}_a\cdot\boldsymbol{r}\right)\int\frac{d\omega_a}{2\pi}G_{2,2}(\boldsymbol{k}_a,\omega_a,-\boldsymbol{k}_a,-\omega_a,\boldsymbol{\kappa},0,-\boldsymbol{\kappa},0). \tag{23}$$

We are interested in the r dependence of this object in the limit $r\kappa\ll1$. To calculate $T_2(r,\boldsymbol{\kappa})$ in this limit we return to Fig. 2(a). Obviously the Gaussian contribution diagram (1) is irrelevant in this limit. The skeleton diagram (2) contributes the following integral:

$$T_2^s(r,\boldsymbol{\kappa})\approx\int\frac{d\omega_a}{2\pi}\int\frac{d\boldsymbol{k}_a}{(2\pi)^3}\,4\sin^2\!\left(\frac{1}{2}\,\boldsymbol{k}_a\cdot\boldsymbol{r}\right)g(k_a,\omega_a)\times g(-k_a,-\omega_a)R_0(\boldsymbol{k}_a,-\boldsymbol{k}_a,\boldsymbol{\kappa},-\boldsymbol{\kappa}), \tag{24}$$

where the tensor indices of the rung were contracted for the longitudinal contribution. The superscript ''s'' is used here and below to denote skeleton contributions. We note that in the limit $k\gg\kappa$ the BL vertices are proportional to the smallest wave vector κ. Thus the rung is proportional to $\kappa^2/k_a^{13/3}$. Integrating over the frequencies of the two Green's functions $g(k_a,\omega_a)$ in this rung [see Eqs. (19), (21)] results in the evaluation $1/[\gamma(k_a)k_a^{13/3}]\propto k_a^{-5}$. Thus the r dependence of T_2^s is given by

$$T_2^s(r,\boldsymbol{\kappa})\propto\int\frac{d\boldsymbol{k}_a}{(2\pi)^3}\,4\sin^2\!\left(\frac{1}{2}\,\boldsymbol{k}_a\cdot\boldsymbol{r}\right)\frac{1}{k_a^5}. \tag{25}$$

Up to logarithmic corrections this integral is proportional to r^2 which is the dissipative solution. Similarly, if we use the bare rung in the diagram in Fig. 2(b) to determine ζ_3 we will find $\zeta_3=3$. In general we will find $\zeta_n=n$ instead of the K41 value of $n/3$. Now one could think that the correct values of the inertial range exponents may be obtained from resumming all the ladder diagrams with the bare rungs. This was the point of view proposed in paper II. In such a case the sought after correction to the scaling exponents is of the order of unity, and it is unclear how to develop a controlled resummation. In this paper we point out a new way, based on the existence of a renormalized rung which gives, upon fusion, K41 exponents *before* ladder resummations. The characteristics of the renormalized rung in such a scheme are dictated by the fusion rules.

Next we want to determine the *renormalized* form of the rung. To this aim we repeat the exercise of integrating over the two Green's functions and the rung, with the vertices determined as before in the limit $k_a\approx k_b\gg\kappa_c\approx\kappa_d$. But now we leave the exponent of k_a in the asymptotic evaluation of the rung free, and *demand* that the result of the integration will be $k_a^{-5/3}$. We find that this requires that $R_0\propto k_a^{-3}$.

We are now in a position to propose a renormalized form of the rung which in a proper calculation could be obtained by summing up all the nonladder diagrams that contribute to this rung. This conforms with our basic hypothesis that all nonladder diagrams contribute to K41, whereas the ladders are responsible for the anomalous scaling. Since K41 does not allow L renormalization we propose the form

$$R^{\alpha\beta\gamma\delta}(\boldsymbol{k}_a,\boldsymbol{k}_b,\boldsymbol{\kappa}_c,\boldsymbol{\kappa}_d) = \delta\overline{\epsilon}^{1/3}\frac{\Gamma^{\alpha\gamma\sigma}(\boldsymbol{k}_a,\boldsymbol{\kappa}_c,\boldsymbol{k}_e)\Gamma^{\beta\delta\sigma}(\boldsymbol{k}_b,\boldsymbol{\kappa}_d,-\boldsymbol{k}_e)}{k_e^3\kappa_c^{2/3}\kappa_d^{2/3}}. \tag{26}$$

This form gives the K41 overall scaling exponent (which is the same as in the bare rung $\boldsymbol{R}_0$, and in addition agrees with the fusion rules for the second-order correlation function with a K41 scaling exponent. In addition it is symmetric, as it should be, for exchanging the indices a and b together with c and d. Note that δ is now a renormalized unknown dimensionless parameter which will be determined later.

To proceed, we note that our actual calculation (see below) depends really only on the asymptotic properties of the rung, which are rigidly determined by the fusion rules. We can thus attempt to simplify the form of the rung as much as

possible, preserving the asymptotic and parity properties unchanged. In particular we note that the BL vertices $\mathbf{\Gamma}(\boldsymbol{k}_a,\boldsymbol{\kappa}_c,\boldsymbol{k}_e)$ have complicated structure which makes calculations involving them rather difficult. Therefore we propose to use instead Eulerian vertices $\boldsymbol{V}(\boldsymbol{k}_a,\boldsymbol{\kappa}_c,\boldsymbol{k}_e)$ corrected by a factor $-2(\boldsymbol{k}_b\cdot\boldsymbol{\kappa}_c)/[k_a^2+k_b^2+\kappa_c^2]$. The correction is aimed at reproducing the asymptotic behavior of the BL vertex $\Gamma^{\alpha\gamma\sigma}(\boldsymbol{k}_a,\boldsymbol{\kappa}_c,\boldsymbol{k}_e)\sim\min\{k_a,k_b,\kappa_c\}$. Thus instead of Eq. (26) one has

$$R^{\alpha\beta\gamma\delta}(\boldsymbol{k}_a,\boldsymbol{k}_b,\boldsymbol{\kappa}_c,\boldsymbol{\kappa}_d) = \frac{-4\delta\overline{\epsilon}^{1/3}(\boldsymbol{\kappa}_c\cdot\boldsymbol{k}_e)(\boldsymbol{\kappa}_d\cdot\boldsymbol{k}_e)}{[k_a^2+\kappa_c^2+k_e^2][k_b^2+\kappa_d^2+k_e^2]} \times\frac{V^{\alpha\gamma\sigma}(\boldsymbol{k}_a,\boldsymbol{\kappa}_c,\boldsymbol{k}_e)V^{\beta\delta\sigma}(\boldsymbol{k}_b,\boldsymbol{\kappa}_d,-\boldsymbol{k}_e)}{k_e^3(\kappa_c\kappa_d)^{2/3}}. \quad (27)$$

As a further simplification of the actual calculations we will use a one-dimensional (1D) reduction of the problem (preserving the asymptotic scaling properties and parity) in which instead of three-dimensional integrations $\int d^3k/(2\pi)^3$ we will use the one-dimensional one $\int_{-\infty}^{\infty}dk/2\pi$. Then we can disregard the vector indices and replace $V^{\alpha\gamma\sigma}(\boldsymbol{k}_a,\boldsymbol{\kappa}_c,\boldsymbol{k}_e)\to k_a$, $(\boldsymbol{k}\cdot\boldsymbol{k}')\to kk'$ (keeping the signs) and k_e^3 in the denominator by $|k_e|$ (because we replaced 3D by 1D integration). The one-dimensional version of the rung (27) turns into

$$R(k_a,k_b,\kappa_c,\kappa_d)=\frac{-4\delta\overline{\epsilon}^{1/3}k_ak_b\kappa_c\kappa_d|k_e|}{[k_a^2+\kappa_c^2+k_e^2][k_b^2+\kappa_d^2+k_e^2]|\kappa_c\kappa_d|^{2/3}}. \quad (28)$$

Note that here $k_a,k_b,\kappa_c,\kappa_d$ are in the interval $\pm\infty$ and that they carry signs in order to preserve the parity of the rungs. Here k_a,k_b are incoming wave vectors and κ_c,κ_d are outgoing, and they conserve momentum

$$k_a+k_b=\kappa_c+\kappa_d. \quad (29)$$

Substituting into Eq. (28) $k_e=k_a-\kappa_c=k_b-\kappa_d$ one finally obtains

$$R(k_a,k_b,\kappa_c,\kappa_d) = -\delta\overline{\epsilon}^{1/3}\frac{k_ak_b\kappa_c\kappa_d|k_a-\kappa_c|}{[k_a^2-k_a\kappa_c+\kappa_c^2][k_b^2-k_b\kappa_d+\kappa_d^2]|\kappa_c\kappa_d|^{2/3}}. \quad (30)$$

In particular,

$$R(k,-k,\kappa,-\kappa)=\frac{-\delta\overline{\epsilon}^{1/3}k^2\kappa^{2/3}|k-\kappa|}{[k^2-k\kappa+\kappa^2]^2}, \quad (31)$$

$$R(k,-k,\kappa,\kappa')=\frac{\delta\overline{\epsilon}^{1/3}\,\mathrm{sgn}(\kappa\kappa')|\kappa\kappa'|^{1/3}}{|k|} \quad \text{for} \quad \kappa,\kappa'\ll k. \quad (32)$$

To check that we get the right K41 scaling exponents with the new renormalized rung we need to recalculate the one-dimensional version of Eq. (24) with (30) for the rung

$$T_2^s(r,\kappa)=\int_{-\infty}^{\infty}\frac{dk}{2\pi}\,4\sin^2\left(\frac{kr}{2}\right)R(k,-k,\kappa,-\kappa) \times\int_{-\infty}^{\infty}\frac{d\omega}{2\pi}g(k,\omega)g(-k,-\omega). \quad (33)$$

Using Eq. (19) the frequency integral yields $-1/2\gamma(k)$. Thus

$$T_2^s(r,\kappa)=\frac{\delta\kappa^{2/3}}{c_\gamma\pi}\int_{-\infty}^{\infty}dk\,\frac{|k|^{4/3}|k-\kappa|\sin^2\left(\frac{kr}{2}\right)}{[k^2-k\kappa+\kappa^2]^2}. \quad (34)$$

In the limit $\kappa\to0$ the integral simplifies to

$$T_2^s(r,\kappa)=2\tilde{\delta}\kappa^{2/3}\int_0^{\infty}\frac{dk}{k^{5/3}}\sin^2\left(\frac{kr}{2}\right), \quad (35)$$

where

$$\tilde{\delta}\equiv\frac{\delta}{\pi c_\gamma}. \quad (36)$$

This integral is elementary, reading

$$T_2^s(r,\kappa)=-\frac{1}{2}\tilde{\delta}(\kappa r)^{2/3}\Gamma\left(-\frac{2}{3}\right)\approx2\tilde{\delta}(\kappa r)^{2/3}, \quad (37)$$

where $\Gamma(x)$ is the gamma function.

The point to notice is that in the asymptotic limit $\kappa\to0$ the only properties of the rung that guaranteed the appearance of the scaling exponent 2/3 are the asymptotic properties that we preserved in the series of simplifications leading to Eq. (30). In general, we will show below that the series of simplifications of the model form of the rung are of absolutely no import also for the calculation of the *anomalous* scaling exponents up to one-loop order. We will show below that we get *precisely* the same exponents in this order with any arbitrary analytic form of the rung, with tensor indices or without, in 3D form or 1D form or whatever, as long as the asymptotics are preserved, as they are. In two-loop order this is no longer true. The actual numbers obtained in the two-loop order are model dependent. We will show, however, that the sensitivity of the predicted exponents ζ_n to the model for the rung is small as long as $n<8$. We need the two-loop order mainly to make sure that it corrects for some unacceptable properties of the one-loop results for higher-order correlation functions.

Before we proceed we need to check the self-consistency of our approach. We need to make sure that all higher-order nonlinear Green's function $\boldsymbol{G}_{p,p}$ (the response of p velocities to p forcing) yield, upon fusion, the correct K41 exponent for pth order correlation functions $\zeta_p^{\mathrm{K41}}=p/3$. For this aim we have to consider the so called *skeleton* diagrams which are the lowest order connected diagrams without loops. For $\boldsymbol{G}_{2,2}$ this is diagram (2) in Fig. 2(a) for $\boldsymbol{G}_{3,3}$ the skeleton contribution are shown as diagrams (3) in Fig. 4(a). We must make sure that the skeleton diagrams, upon fusion, yield K41 scal-

ing $\zeta_p^{\rm K41}=p/3$ for the appropriate pth-order correlation functions, since our grand hypothesis is that the anomalous scaling comes only from ladder resummations.

This test of self-consistency is presented in Appendix B. The important conclusion of this appendix is that the skeleton diagrams for $G_{p,p}(\{k_j,\kappa_j\})$ (with asymptotics of the rung defined by the two-point fusion rules with $\zeta_2^{\rm K41}=2/3$) automatically reproduces the K41 scaling exponent $\zeta_p^{\rm K41}=p/3$ when p points are fused.

V. SANDING THE FLOOR IN ONE-LOOP ORDER

In this section we demonstrate the most important new property of the resummed theory, i.e., that the rungs in the ladder diagrams appear with a small parameter. This will allow us to develop a *controlled* ladder resummation, something that to our knowledge has never been available before. In fact, we will lay out in this section all that is needed to calculate the scaling exponents in the one-loop order. In Sec. V A we demonstrate that the prefactor δ of the rung is the order of δ_2 which is the anomalous part of ζ_2 and thus small. In Sec. V B we consider the anomalous exponent of the rung itself, denoted as δ_a, and stemming from ladder resummations within the rung infinite series representation. In Sec. V C we reconsider the contribution of the skeleton diagrams to the scaling exponents upon fusion, taking into account the anomaly of the rung. In Sec. V D we throw in the following input: the fact that $\zeta_3=1$ and the experimental value of ζ_2. The result is Eq. (60) which states that in the one-loop order all the unknown parameters are numerically identical. From this point the calculation of all the other scaling exponents in one-loop order is straightforward.

A. The four-point rung is small

Here we show that the coefficient δ in front of the renormalized four-point rung (26) is of the order of the correction to K41 of the scaling exponent ζ_2

$$\delta_2=\zeta_2-\zeta_2^{\rm K41}\approx 0.03. \tag{38}$$

To this aim consider the one-dimensional version of the quantity $T_2(r,\boldsymbol{\kappa})$ of Eq. (23):

$$T_2(r,\kappa)=\int_{-\infty}^{\infty}\frac{dk_a}{2\pi}\,4\sin^2\!\left(\frac{1}{2}k_a r\right)\int_{-\infty}^{\infty}\frac{d\omega_a}{2\pi}G_{2,2}(k_a,\omega_a,-k_a,-\omega_a,\kappa,0,-\kappa,0). \tag{39}$$

We will examine the ratio of the contributions of the one-loop diagram (3), denoted below as $T_2^{(1)}(r,\kappa)$, to the contribution of the skeleton diagram Eq. (33) [diagram (2) in Fig. 2(a)]. After performing the frequency integrals the one-dimensional form of $T_2^{(1)}(r,\kappa)$ [see diagram (3) in Fig. 2(a)] is

$$T_2^{(1)}(r,\kappa)=\int_{-\infty}^{\infty}\frac{dk_a}{\pi\gamma(k_a)}\sin^2\!\left(\frac{1}{2}k_a r\right)\int_{-\infty}^{\infty}\frac{dq}{2\pi\gamma(k_a)}\times R(k_a,-k_a,q,-q)R(q,-q,\kappa,-\kappa). \tag{40}$$

In the asymptotic limit defined by $\kappa r\to 0$ the main contribution to the integral comes from the two symmetric regions of the q integration in which $|\kappa|\ll|q|\ll|k_a|$. In these regions we use the form (32). We calculate

$$T_2^{(1)}(r,\kappa)\approx 2\tilde{\delta}^2\kappa^{2/3}\int_0^{\infty}\frac{dk_a}{k_a^{5/3}}\sin^2\!\left(\frac{1}{2}k_a r\right)\int_{\kappa}^{k_a}\frac{dq}{q}. \tag{41}$$

As expected the loop integral over q produces a logarithmic contribution. At this point we use the asymptotical identity

$$\lim_{\kappa r\to 0}\int_0^{\infty}d(kr)f(kr)\ln\!\left(\frac{k}{\kappa}\right)=\ln\!\left(\frac{1}{r\kappa}\right)\int_0^{\infty}d(kr)f(kr), \tag{42}$$

which produces, upon comparison with Eq. (35) the final result

$$T_2^{(1)}(r,\kappa)=\tilde{\delta}\ln\!\left[\frac{1}{\kappa r}\right]T_2^{(s)}(r,\kappa). \tag{43}$$

The factor $\tilde{\delta}$ that was introduced in Eq. (36) reappears here in front of the logarithm as the effective parameter of expansion.

Analogously one computes the leading contribution of the two-loop diagram (4) in Fig. 2(a). This is done explicitly in Secs. VII A and Appendix C,

$$T_2^{(2)}(r,\kappa)=\frac{1}{2}\left[\tilde{\delta}\ln\!\left(\frac{1}{r\kappa}\right)\right]^2 T_2^{(s)}(r,\kappa), \tag{44}$$

and, in general the leading contribution of the n-loop diagram

$$T_2^{(n)}(r,\kappa)=\frac{1}{n!}\left[\tilde{\delta}\ln\!\left(\frac{1}{r\kappa}\right)\right]^n T_2^{(s)}(r,\kappa). \tag{45}$$

The sum of all these contributions is as follows:

$$T_2(r,\kappa)=T_2^{(s)}(r,\kappa)+\sum_{m=1}^{\infty}T_2^{(m)}(r,\kappa) \tag{46}$$

$$=T_2^{(s)}(r,\kappa)\sum_{m=0}^{\infty}\frac{1}{m!}\left[\tilde{\delta}\ln\!\left(\frac{1}{r\kappa}\right)\right]^m=\frac{T_2^{(s)}(r,\kappa)}{(r\kappa)^{\tilde{\delta}}}.$$

We see that, as usual, resummation of the leading contributions from the logarithmic ladder diagrams results in the power function with the exponent $\tilde{\delta}$ which is the prefactor of the logarithm in the one-loop diagram, see Eq. (43). Because the expected correction δ_2 to the K41 exponent $\zeta_2^{\rm K41}$ is small ($\delta_2\approx 0.03$) we conclude that the prefactor of the rung $\tilde{\delta}$ is small as well. This allows us to begin with the one-loop approximation in computing the higher-order scaling exponents ζ_p with $p>2$.

B. Anomalous correction of the rung asymptotics

So far we have disregarded the explicit appearance of ladder diagrams in the infinite series that defines the rung itself. As pointed out in paper II the same kind of ladder

resummation that is responsible for the anomaly of the exponents of the nonlinear Green's functions will also contribute an anomalous part to the scaling properties of the rung. Nevertheless the outer and inner scale do not appear in the rung either, and therefore the anomaly is explicit only in the asymptotic regime where we have a ratio of large and small scales. In this section we flush out this anomaly.

Instead of Eq. (32) we expect

$$R_a(k,-k,\kappa,\kappa') = \frac{\delta\overline{\epsilon}^{1/3}\,\mathrm{sgn}(\kappa\kappa')|\kappa\kappa'|^{1/3+\delta_a}}{|k|^{1+2\delta_a}} \quad \text{for} \quad k \gg \kappa,\kappa', \tag{47}$$

with some anomalous exponent δ_a which is expected (and later demonstrated) to be of the order of $\tilde{\delta}$ as it stems from the same origin. This correction to the asymptotics may be achieved, for example by the following model form of the rung (30):

$$R_a(k_a,k_b,\kappa_c,\kappa_d) = R(k_a,k_b,\kappa_c\kappa_d)\left(\frac{|\kappa_c\kappa_d|}{|k_a-\kappa_c|^2}\right)^{\delta_a}. \tag{48}$$

As before, we will argue that the exact analytic form of the rung is not important for our calculations, and only the asymptotic scaling form is essential. This statement will be shown to be exact in the one-loop order. We thus need at this point only to preserve the essential properties, i.e., that the outer scale L cannot appear due to locality, that the rung has to be symmetric with respect $a,b\to c,d$, etc.

C. Contributions of the skeleton diagrams with the anomalous four-point rung

In this section we reconsider the skeleton diagrams appearing in the nonlinear Green's functions $G_{p,p}$ but taking into account the anomaly of the rung. In other words we are going to compute the scaling exponents accounting only for the ladder resummation *inside* the rung, but not the ladder resummation with the anomalous renormalized rungs. This final step will be done in Secs. VI and VII.

We are interested in the scaling exponents of structure functions in r representation, and these are obtained from the correlation functions in k representation as detailed in Appendix B. Upon fusion we obtain automatically contributions behaving as nonliner Green's functions. Accordingly the objects of interest in the analysis below are the nonlinear Green's functions in which the k dependence of the fusing coordinates is transformed to r representation. The outgoing wave vectors κ are left as are, and the outgoing frequencies can be put to zero with impunity. This results in objects defined in a mixed r,κ representation, which we denote as $T_p(r,\{\kappa_j'\})$:

$$T_p(r,\{\kappa_j'\}) = \int_{-\infty}^{\infty}\prod_{i=1}^{p}\frac{d\omega_i dk_i}{(2\pi)^2}\,\delta(\omega_1+\cdots\omega_p)\times\delta(k_1+\cdots k_p)f_p(r,\{k_j\})\times G_{p,p}(\{k_j,\omega_j,\kappa_j,0\}). \tag{49}$$

Here $f_p(r,\{k_j\})$ are one-dimensional versions of the functions $f_p(\boldsymbol{r},\{\boldsymbol{k}_j\})$ defined by Eq. (B7). The set $\{\kappa_j\}$ denotes all the outgoing wave vectors.

We consider the skeleton contributions to the nonlinear Green's function $G_{p,p}$, denoted by $G^s_{p,p}$. Similarly to the definition (33) we introduce $T^s_p(r,\{\kappa_j\})$ as

$$T^s_p(r,\{k_j'\}) = \int_{-\infty}^{\infty}\prod_{i=1}^{p}\frac{d\omega_i dk_i}{(2\pi)^2}\,\delta(\omega_1+\cdots\omega_p)\times\delta(k_1+\cdots k_p)f_p(r,\{k_j\})\times G^s_{p,p}(\{k_j,\omega_j,\kappa_j,0\}). \tag{50}$$

Repeating the calculation of Appendix B in the asymptotic regime $\kappa_j r\ll 1$ but with the redefined rung (47) one gets

$$T_p(r,\{\kappa_j\}) = C_p(\overline{\epsilon}r)^{p/3}r^{p\delta_a}\prod_{j=1}^{p}|\kappa_j|^{1/3+\delta_a}. \tag{51}$$

Here C_p are dimensionless constants that absorb all the numerical factors. In fact, the result (51) could be guessed directly by recognizing that every rung which is connected with the ''outgoing'' Green's functions $G(\kappa_j,0)$ contributes to $T_p(r,\{\kappa_j\})$ a factor $|\kappa_j|^{1/3+\delta_a}$. All together they give $\Pi_{j=1}^{p}|\kappa_j|^{1/3+\delta_a}$. Convergence of the integrals over κ_j and ω_j implies that neither inner nor outer scales may appear, and therefore dimensional consideration require a factor $r^{p(1/3+\delta_a)}$.

D. The second and third order correlation functions: relations between δ_a, δ_2, and $\tilde{\delta}$

Consider first the scaling exponent ζ_2. In Sec. V A we showed that the resummation of the ladder diagrams leads to an anomalous correction to the exponent $\zeta_2^{\mathrm{K41}}=\frac{2}{3}$ which is $-\tilde{\delta}$ [see Eq. (46)]. But according to Eq. (51) the ladder in the skeleton contribution brings in an additional correction $2\delta_a$. Altogether we have in the one-loop order

$$\zeta_2 = \tfrac{2}{3} - \tilde{\delta} + 2\delta_a. \tag{52}$$

Therefore the exponent δ_2 defined by Eq. (38) may be expressed as follows:

$$\delta_2 = 2\delta_a - \tilde{\delta}. \tag{53}$$

Another relation between the exponents will follow from the analysis of the fusion of three points. To one-loop order the nonlinear Green's function $G_{3,3}$ has the skeleton contribution diagram 3 in Fig. 4(a), and the one-loop diagrams in Fig. 4(b). The skeleton contribution can be read directly from Eq. (51):

$$T^s_3(r,\{\kappa_j\}) = C_3\overline{\epsilon}r r^{3\delta_a}|\kappa_1\kappa_2\kappa_3|^{1/3+\delta_a}. \tag{54}$$

To discuss the other contributions we refer to Fig. 4 in which all the diagram of $G_{3,3}$ with zero, one and two rungs are represented. We have one diagram with no rung, three with one, nine with two. The multiplicity of 3 in the diagrams of type (2) represent the three possible connections of two struts by two rungs. The multiplicity of 6 in the diagrams of type

(3) represent the different pair permutations of three struts. In general there are 3^n diagrams with n rungs, out of which three will have one disconnected strut. Diagrams with disconnected struts will not contribute in the asymptotic regime that interests us here. Thus out of the diagrams in Fig. 4(a) only the skeleton diagram (3) remains in the asymptotic regime.

In general, with n rungs we have 3^n-3 fully linked diagrams. This number is $6[(3^{n-1}-1)/2]$, and the number $[(3^{n-1}-1)/2]$ counts the topologically distinct fully linked diagrams with n rungs. Thus for example we represent in Fig. 4(b) the four topologically distinct contributions with three rungs. These are all the one-loop ladder diagrams contributing to the third-order correlation function. We show now that of these four terms diagram (1a) does not contribute a logarithmic divergence, whereas the other three contribute the same logarithmic term. In fact, this is the beginning of a systematic rule: the only diagrams that contribute logarithmic terms in the one-loop order are those in which the last rung appears to the right of the skeleton diagrams. Similar rules will be established below for higher-loop contributions.

Consider then the one-loop diagram (1a) in Fig. 4(b) in which this rule is not obeyed. We focus on the loop made by the two rungs and the Green's functions q and q', considering the asymptotic regime $k_a, k_b \gg q \gg \kappa_a, \kappa_b$. This is the only regime in which a logarithmic divergence is possible. In this regime $q' \approx q'' \approx k_a + k_b$. Thus the rung $R_a(k_a, k_b, q, q')$ contributes to the loop $q^{1/3+\delta_a}$. The rung $R_a(q, q', \kappa_a, q'')$ and the Green's function $G(q')$ do not contribute any q dependence to the integrand. The ω integration over the product of the Green's functions $G(q)$ and $G(q')$ gives approximately $1/\gamma(q')$ and again contributes no q dependence. Finally we have the evaluation

$$T_3^{(1a)} \propto \int_{\kappa}^{k_a} dq q^{1/3+\delta_a}. \tag{55}$$

Clearly, this diagram does not exhibit a logarithmic divergence and as such it does not contribute to the renormalization of the scaling exponent.

The other three diagrams in Fig. 4(b) [namely, (1b), (1c), and (1d)] are different, they all have a logarithmic divergence. The reason for the difference is that in these three diagrams there are four Green's functions, instead of five in diagram (1a), which carry large wave vectors. This is the same situation as in the skeleton diagram (3) in Fig. 2(a). In the loop we have now two Green's functions, instead of one in diagram (1a), that carry small wave vectors q. This difference leads to a different q dependence in the loop, and to a logarithmic divergence. We demonstrate this explicitly in the next paragraph, but we already draw the conclusion which is general: one-loop ladder diagrams with logarithmic divergences are those in which the additional rung (compared to skeleton diagram) has been positioned to the *right* of the skeleton structure.

Explicitly, consider diagram (1b) in Fig. 4(b). The rung $R_a(k_a, k_b, q, q')$ contributes $q^{1/3+\delta_a}$ as before. But now also the rung $R_a(q', k_c, -q, \kappa_c)$ contributes the same q dependence. On the other hand, the rung $R_a(q, -q, \kappa_a, \kappa_b)$ contributes $|q|^{-1-2\delta_a}$. The ω integration with the product of the two Green's functions $G(q,\omega)G(-q,-\omega)$ is the same as Eq. (33) leading to $-1/2\gamma(q)$. In total we have a logarithmic integral.

The diagram (1d) is very similar to (1b); it has the same rung structure at the left, and the rightmost rung is $R_a(q, -q, \kappa_a, \kappa_c)$. This makes no difference to the q dependence and thus to the logarithmic divergence or to the factor in front of the logarithm. Diagram (1c) is slightly different, having the third rung on the same ladder as the second rung. Nevertheless the rung $R_a(q', k_c, q, -q)$ contributes exactly the same q dependence as the *two* rungs in diagrams (1b) or (1d). Thus it yields at the end the same factor with the same logarithm. Finally, comparing (1c) to diagram (3) in Fig. 2(a) we see that the loop structures are identical in both, and thus if diagram 3 had a prefactor $\tilde{\delta}$, we can immediately conclude that the *three* diagrams [(1b), (1c), and (1d)] will result in a total prefactor of $3\tilde{\delta}$:

$$T_3^{(1)}(r, \{\kappa_j\}) = 3\tilde{\delta} \ln\left[\frac{1}{r\kappa}\right] T_3^{(s)}(r, \{\kappa_j\}), \tag{56}$$

where $\kappa \equiv [\kappa_1 \kappa_2 \kappa_3]^{1/3}$. The leading contribution from the higher loop diagrams can be seen to contribute higher order terms in the series of a power law, similarly to the mechanism displayed in Eqs. (43)–(46):

$$T_3(r, \{\kappa_j\}) = \frac{T_3^{(s)}(r, \{\kappa_j\})}{[r\kappa]^{3\tilde{\delta}}}. \tag{57}$$

Substituting Eq. (54) we find finally

$$T_3(r, \{\kappa_j\}) = C_3 \overline{\epsilon} [r\kappa]^{1+3\delta_a - 3\tilde{\delta}}. \tag{58}$$

Accordingly to one-loop order we write

$$\zeta_3 = 1 + 3\delta_a - 3\tilde{\delta}. \tag{59}$$

At this point we use the exact, nonperturbative result that $\zeta_3 = 1$ to find the relationship between δ_a and $\tilde{\delta}$: $\delta_a = \tilde{\delta}$. Together with Eq. (53) we get the important conclusion that all our δ's are the same:

$$\delta_2 = \delta_a = \tilde{\delta} = \zeta_2 - \zeta_2^{\mathrm{K41}} \approx 0.03. \tag{60}$$

We should stress that this important result is obtained using only the asymptotic scaling properties of the rung. Changing the explicit form of the rung without ruining the asymptotics will affect only the subleading terms in the analysis. The leading logarithmic terms are insensitive to the details of the analytic form of the rung.

VI. ANOMALOUS SCALING EXPONENTS IN THE ONE-LOOP APPROXIMATION

We are poised to compute now the anomalous corrections to all the scaling exponents of the p-order correlation functions in the one-loop approximation. Start with the fourth-order nonlinear Green's function, and consider the skeleton diagrams in Fig. 5. In the one loop order, to obtain a logarithmic divergence in the asymptotic regime we must add the additional rung *on the right* of the skeleton structure. The

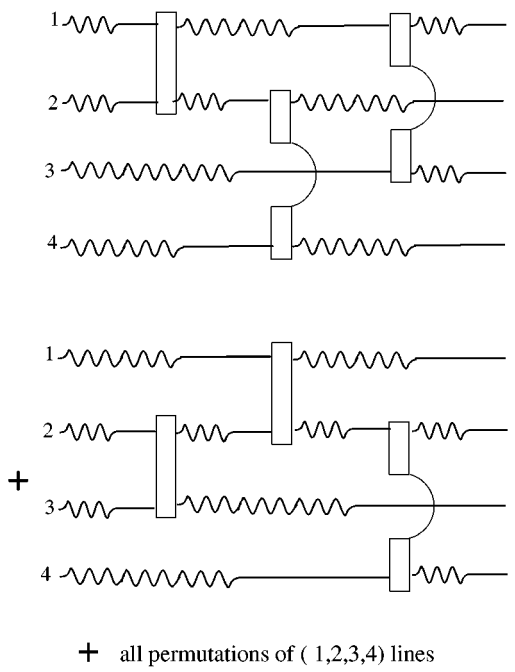

FIG. 5. The skeleton contributions in the diagrammatic expansion of $\mathbf{G}_{4,4}$.

combinatorics are elementary: Each skeleton diagram can host a new rung on the right in six different ways. Once a rung has been put in place the leading (logarithmic) contribution to the loop integral is the same as the loop integrals considered in the last section. It gives the same logarithm *with the same prefactor*. The only difference is in the combinatorics. We can thus write by inspection

$$T_4^{(1)}(r,\{\kappa_j\}) = 6\tilde{\delta}\ln\left[\frac{1}{r\kappa}\right]T_4^{(s)}(r,\{\kappa_j\}), \tag{61}$$

where κ is the geometric mean of all the κ_j. Resumming the leading contributions of the higher-order loop diagrams results in the power law

$$T_4(r,\{\kappa_j\}) = \frac{T_4^{(s)}(r,\{\kappa_j\})}{[r\kappa]^{6\tilde{\delta}}}. \tag{62}$$

Using Eq. (51) we reach the final result

$$\zeta_4 = 4/3 + 4\delta_a - 6\tilde{\delta} = 4/3 - 2\delta_2, \quad \text{one-loop order.} \tag{63}$$

The analysis of the one-loop-order contribution to the anomalous exponents of the p-order correlation functions is as straightforward. There are $p(p-1)/2$ possibilities to append an additional rung to the right of the skeleton structure of the p-order nonlinear Green's function. All these diagrams contribute identical leading order logarithmic terms, with the same prefactor, summing up to an anomalous correction to the scaling exponent of the skeleton diagrams which is $\tilde{\delta}p(p-1)/2$. According to Eq. (51) the scaling exponent of the skeleton contribution itself is corrected with respect to K41 by $p\delta_a$. Thus altogether

$$\zeta_p = \frac{p}{3} + p\delta_a - \tilde{\delta}\frac{p(p-1)}{2}. \tag{64}$$

Using Eq. (60)

$$\zeta_p = \frac{p}{3} - \delta_2\frac{p(p-3)}{2}, \quad \text{one-loop order.} \tag{65}$$

We note that this formula, which is valid in our case to one-loop order only, is identical in prediction to Kolmogorov's log-normal phenomenological model (known as K62). This is interesting, as it stems from the nontrivial topology of the ladder diagrams, in which only the most leading were considered. In other words, there are many diagrams without logarithmic divergences, but when we resum those that do have logarithms in the leading order we find K62. The present authors find the connection between lognormality and ladder diagrams unexpected.

Nevertheless we should recognize that in the present approach this result has a limited region of validity. The analysis of the two-loop order which is provided below will show that Eq. (4) is only valid when $p\delta_2 \ll 1$. The two-loop order will contribute *positive* terms of the order of $\delta_2^2 p^2(p-3)$, *reducing* the negative tendency of the correction to K41. Accordingly the present theory will not suffer from the well know deficiencies of the K62 log-normal model which for us is only a first order result.

VII. ANOMALOUS SCALING EXPONENTS IN THE TWO-LOOP APPROXIMATION

In this section we calculate the two-loop contributions to the scaling exponents ζ_p. Even though these contributions are very small when $p\delta_2$ is small (for, say, $p<6$), they become important for larger values of p where K62 begins to turn down the n dependence of ζ_n. In addition this calculation allows to present clear ranges of validity for the one-loop and two-loop calculations.

A. Two-loop contributions to ζ_2

We consider the two-loop diagram (4) in Fig. 2(a). Substituting it instead of $G_{2,2}$ in Eq. (39) we obtain the quantity $T_2^{(2)}(r,\kappa)$. We want to compute the correction that this diagram gives to the skeleton diagram (2), and to this aim we divide it by $T_2^s(r,\kappa)$. In the asymptotic regime $\kappa r \ll 1$ the loop integrals over q_1 and q_2 contribute mostly in the range $k \gg q_1, q_2 \gg \kappa$. In this regime the integrals over k_a, ω_a cancel from the ratio of $T_2^{(2)}(r,\kappa)/T_2^s(r,\kappa)$. In addition the Green's functions $G(\kappa_c)$ and $G(\kappa_d)$ cancel. Thus this ratio can be read from the ratio of the corresponding diagrams for $G_{2,2}$, or taking the diagram (4) and amputating the incoming and outgoing legs. We still need to divide by the rung in diagram (2) where k_a is replaced by $1/r$:

$$\frac{T_2^{(2)}(r,\kappa)}{T_2^s(r,\kappa)} = \frac{1}{R(1/r,-1/r,\kappa,-\kappa)}\int_{-\infty}^{\infty}\frac{dq_1 dq_2 J(q_1)J(q_2)}{(2\pi)q_1 q_2} \times R(r^{-1},-r^{-1},q_1,-q_1)R(q_1,-q_1,q_2,-q_2) \times R(q_2,-q_2,\kappa,-\kappa),$$

$$J(q)=\int_{-\infty}^{\infty}\frac{d\omega}{2\pi}G(q,\omega)G(-q,-\omega)=-\frac{1}{2\gamma(q)}. \quad (66)$$

In Appendix C we analyze this integral in the asymptotic limit $\kappa r\ll 1$ with the final result

$$T_2^{(2)}(r,\kappa)=\tilde{\delta}^{\,2}\left[\frac{1}{2}\ln^2\left(\frac{1}{\kappa r}\right)+b_1\ln\left(\frac{1}{\kappa r}\right)\right]T_2^s(r,\kappa), \quad (67)$$

where b_1 is a dimensionless constant

$$b_1\approx -0.434. \quad (68)$$

In Eq. (67) the $\ln^2$ term accounts for the exponentiation of the one-loop contribution, whereas the ln term provides the two-loop correction to the scaling exponent ζ_2. Instead of Eq. (53) we now read

$$\delta_2=2\delta_a-\tilde{\delta}-b_1\tilde{\delta}^2. \quad (69)$$

A second relation between these exponents will be derived in the next section.

B. Two-loop contributions to ζ_3

The calculation to $O(\delta_2^2)$ of the contributions to ζ_3 and of higher-order ζ_p due to ladder resummations introduces six-point irreducible interactions amplitudes. These appear in the ladder diagrams as rungs with six legs, arising from diagrams that due to their topology cannot be resummed into reducible contributions consisting of two four-point rungs and one Green's function. The six-point rung is discussed in Appendix F. In particular we explained there why the *functional dependence* of ζ_p on p can be understood completely on the basis of the analysis of ladders with four-point rungs. This stems from the fact that the reducible and irreducible contributions to the six-point rung are of the same order, and their combinatorical factors are identical.

There are many possible two loop diagrams involving four-point rungs that appear in the expansion of $G_{3,3}$. However, we are only interested in those contributing a logarithmic divergence in the asymptotic regime. As before, to get the relevant diagrams we need to append the last rung *to the right* of the existing one-loop structure. Thus, we begin with the three logarithmic diagrams in Fig. 4(b) [i.e., (1b), (1c), and (1d)] and consider all the diagrams that are obtained by adding an additional rung on the right which connects two struts. The nine resulting diagrams are shown in Appendix E. These diagrams are subdivided into two groups: three diagrams in which the last rung connects the same struts as the previous rung, and six diagrams in which the last rung connects different struts. In Appendix E we explain that the first group of diagrams gives exactly the same asymptotic integral as the two-loop contribution to ζ_2. This statement should be reiterated because of its importance to the structure of the theory: the integrals are different, but once the limits $k\gg q_1,q_2\gg\kappa$ are taken, the resulting integrals coalesce with those computed in the previous section. Thus the contribution to ζ_3 from these three diagrams will be $3b_1\tilde{\delta}^2$ (which is three times larger than the corresponding contribution to ζ_2).

The six diagrams of the second group look topologically different, but again in the asymptotic regime coalesce into an identical integral Eq. (D1) with $\tilde{\Psi}\to\tilde{\Psi}_2$, where

$$\tilde{\Psi}_2(q_1,q_2)=\frac{q_1|q_1|^{1/3}|q_1+q_2|^{4/3}\,\mathrm{sgn}(q_2)}{(|q_1|^{2/3}+|q_2|^{2/3}+|q_1+q_2|^{2/3})(q_1^2+q_2q_1+q_2^2)}. \quad (70)$$

Following the procedure outlined in Appendix D we find the coefficients of expansion

$$a_2=1, \quad b_2\approx -0.55. \quad (71)$$

Finally we get the two-loop form of ζ_3:

$$\zeta_3=1+3\delta_a-3\tilde{\delta}-\tilde{\delta}^2(3b_1+6b_2). \quad (72)$$

Demanding again $\zeta_3=1$ we find from Eqs. (69), (72)

$$\tilde{\delta}=\delta_2-(b_1+4b_2)\delta_2^2+O(\delta_2^3), \quad (73)$$

$$\delta_a=\tilde{\delta}\,[1+(b_1+2b_2)\tilde{\delta}]. \quad (74)$$

These results are used in the next section to calculate ζ_n for $n\geqslant 3$ to two-loop order.

C. Two-loop contributions to ζ_p, $p\geqslant 4$

The calculation of the contribution of four-point rungs to ζ_p for higher values of p does not necessitate the evaluation of new integrals. In Appendix E we explain that all the two-loop integrals appearing in the ladders of $G_{4,4}$ and higher-order nonlinear Green's functions are identical in the asymptotic regime to one of the two integrals appearing in the three-order quantity. The only differences are in the combinatorial factors that account for how many ways we can choose the rungs to connect between p struts.

If the second rung is connecting the same struts as the rung before it we have the same combinatorial factor as in the one-loop order, namely, $p(p-1)/2$. This provides a contribution to ζ_p which is $p(p-1)\tilde{\delta}^2b_1/2$. If the second rung is *not* connecting the same struts as the rung before it, we have $p(p-1)(p-2)$ contributions. This is due to the existence of $p(p-1)/2$ ways connect two struts with the first rung, and then $2(p-2)$ ways to connect one of these two struts with the remaining $(p-2)$ struts. This leads to a contribution $p(p-1)(p-2)b_2\tilde{\delta}^2$. We should stress that the loops must have a joint strut to give a ln contribution. Two disconnected loops lead only to $\ln^2$ contributions, which do not enter the two-loop corrections to the scaling exponents. In total we find

$$\zeta_p=\frac{n}{3}+p\delta_a-\frac{p(p-1)}{2}[\tilde{\delta}+b_1\tilde{\delta}^2]-p(p-1)(p-2)b_2\tilde{\delta}^2+O(\tilde{\delta}^3). \quad (75)$$

Substituting Eqs. (73), (74) we obtain finally

$$\zeta_p=\frac{p}{3}-\frac{p(p-3)}{2}\delta_2[1+2\delta_2b_2(p-2)]+O(\delta_2^3). \quad (76)$$

We should stress that the functional form presented in this equation is solid. It is shown in Appendix F that the contribution coming from six-point irreducible rungs is only renormalizing the value of b_2 which anyway depends on the precise analytic form of the four-point rung which is not available at the present time. We estimate the range of validity of this order of the calculation by the Hölder inequalities, which disallow a nonlinear increase in the ζ_p as a function of p. The inflection point where this requirement is violated may serve as a good estimate for the range of validity. This inflection point occurs at $p \approx 1.4 - 1/(6 b_2 \delta_2) \approx 12$. In Fig. 1 we show, within this range, the K41 prediction, the one-loop approximation (equivalent to K62) and our two-loop final result. It is obvious that the two-loop loop prediction goes considerably beyond the range of validity of the K62 formula which has an unphysical maximum at $p \approx 11.5$. We believe that all the reliably measured values of ζ_p agree very well with this prediction.

Using the bridge relation [7] $\mu = 2 - \zeta_6$ we predict

$$\mu = 9 \delta_2 (1 + 8 b_2 \delta_2). \tag{77}$$

Plugging in the numbers we get $\mu = 0.235 + O(\delta_2^3)$. This is to be contrasted with the K62 prediction $\mu \approx 0.27$. We conclude that the two-loop contribution is very significant for experimentally measured exponents. If one wishes to obtain theoretical results for ζ_p with higher values of p one needs to consider the three-loop contributions, which pose no further conceptual difficulties. Nevertheless the experimental situation does not warrant at the present time the effort needed to accomplish such a calculation.

One should stress before closing this section that the form of Eq. (76) is universal, stemming from the structure of the ladder diagrams and from combinatorics only. However, the numerical value of b_2 is model dependent. We have checked that changing the form of the rung keeping the asymptotics unchanged results in b_2 remaining negative while its value not changing by more than a factor of 2 or so. At this moment in time one can determine b_2 using the value of ζ_4 from experiments, allowing us then to predict accurate values of ζ_n for n up to 12. It is our plan, however, to develop in the near future a theoretical equations for the four-point and six-point rungs, leading to an *ab initio* determination of their analytic forms, and with them of the parameters $\tilde{\delta}$ and b_2.

VIII. SUMMARY AND DISCUSSION

The main steps of this and previous papers leading to the present results have been as follows.

The theory is developed using BL velocities to eliminate the spurious infrared divergences that are due to sweeping effects when Eulerian velocities are employed.

The Dyson-Wyld perturbation theory was line resummed in order to achieve order-by-order convergent perturbation theory with K41 propagators as the lines in the theory. At this point the objects of the theory are two two-point propagators (Green's function and correlator) and one three-point vertex. The three-point vertex is in no way ''small,'' and renormalizing it does not change this fact [27].

Multipoint correlation functions are considered when p coordinates coalesce together. In the fusion limit $\kappa r \to 0$ it is advantageous to reorganize the theory in terms of one propagator (K41 Green's function), and four-point, six-point vertices, etc. (the rungs). The series of diagrams contributing to the fusion limit are then simple ladder diagrams.

The crucial step of the theory is achieved by two requirements: (i) the four-point rung should be consistent at the level of the *skeleton diagrams* with the fusion rules with K41 scaling exponents. (ii) The resummation of the ladder diagrams that appear when two coordinates fuse together should lead to the *correct* value of ζ_2. These double requirements accomplish two things at once: (a) the theory is now developed *around the K41 limit*, leading to the appearance of the small parameter δ_2 in front of the four-point rung and (b) all the anomalies are coming from the ladder resummations. The six-point rung is shown explicitly (Appendix F) to be of second order in the small parameter, eight-point rungs are of third order, etc.

We computed the anomalous exponents in one-loop order, inputting the value of ζ_2 and requiring that $\zeta_3 = 1$. The result is that the scaling exponents are predicted to this order to agree with the log normal model K62. We showed that to this order the result is universal, independent of the simplifications and of the model form of the rung.

We computed the anomalous exponents in two-loop order. The difficulty of K62 is overcome, the two-loop contribution has a sign that lifts up the exponents from the down curve of the K62 parabola. While the form of the two-loop result is universal, the numerical value of the parameter b_2 appearing in the final result is model dependent, with contributions for the four-point and six-point rungs.

For the reader who is more trained in renormalized perturbation theory we should remark at this point that this paper represents an additional conceptual development compared to the point of view proposed in papers II and III. In those papers the rungs in the ladder were left undressed. As shown in Sec. IV A the undressed rungs lead to viscous scaling of the skeleton diagrams ($\zeta_n = n$). Accordingly, if one does not dress the vertices, the ladder resummation for $\boldsymbol{G}_{2,2}$ should result in renormalizing the exponent ζ_2 all the way from 2 to about 2/3. This amounts to having δ_2 of the order of 4/3. While this was considered as a possibility in papers II and III the present development casts strong doubts on this scenario. Indeed, considering ζ_3 for example the same scenario gives in the one-loop order $\zeta_3 \approx -1$ instead of the required $+1$. This may be salvaged by requiring the full six-point rung. But this will make the dimensionless coefficient of the six-point rung of the order of 2. Now one will run into even worse troubles with ζ_4 in two-loop order, requiring an even bigger coefficient for the eight-point rung. Correspondingly every higher-order scaling exponent will require a bigger and bigger n-point rung, without hope of analytic form for ζ_n. We propose that the present scenario offers simplicity and elegance that appears very attractive.

To improve upon the present theory one needs to develop a theory for the four-point and six-point interaction amplitudes. Here we determined only the asymptotic properties of the four-point rung, and this allowed us to predict the form of the scaling exponents, but an input of the value of the anomalous part of ζ_2 was needed to achieve one-loop order. In fact we could use the value of ζ_4 to fix the value of b_2 and

gain a solid prediction of all the exponents to two-loop order. Such a prediction for ζ_n would be valid up to $n \approx 12$. It is very easy to generalize the result that we have to three-loop order, with the introduction of yet one more parameter associated with the three-loop integrals, say b_3, which included also contributions from the irreducible eight-point rung. The result would read

$$\zeta_n = \frac{n}{3} - \frac{n(n-3)}{2}\delta_2[1 + 2\delta_2(n-2)b_2 + 6\delta_2^2 b_3(n-1)(n-2)] + O(\delta_2^4). \tag{78}$$

We stress that this form stems from the structure of the ladder diagrams, and we consider it very solid. From one point of view we can now use the value of ζ_5 to fix b_3 to provide a prediction that is valid for any n within experimental reach for quite some time. But this is not the main point. The main point is that we have identified the coefficients appearing in this formula with particular objects, i.e., the four-point and higher-order vertices which appear in the theory as the rungs of the ladders. Obviously, a calculation of the renormalized rungs from first principle would remove the need to input experimental information altogether, affording us a complete theory of the scaling exponents of isotropic turbulence. At this point this is still not available.

ACKNOWLEDGMENTS

It is a pleasure to thank Anna Pomyalov for her patient help with the diagrams in this paper. We thank her, Yoram Cohen, Ayse Erzan, Chris Stephens, and Massimo Vergassola for useful comments on the manuscript. This work was supported in part by the Israel Science Foundation, the German-Isreali Foundation, the European Commission under Contract No. HPRN-CT-2000-00162 (''Nonideal Turbulence''), and the Naftali and Anna Backenroth-Bronicki Fund for Research in Chaos and Complexity.

APPENDIX A: RESUMMATION INTO DIAGONAL K41 PROPAGATORS

The starting point of this rearrangement are the mass operators in k,ω representation $\Sigma_{\alpha\beta}(\boldsymbol{r}_0|\boldsymbol{k}_1,\boldsymbol{k}_2,\omega)$ and $\Phi_{\alpha\beta}(\boldsymbol{r}_0|\boldsymbol{k}_1,\boldsymbol{k}_2,\omega)$. Define the ''diagonal'' part of the mass operators as

$$\sigma_{\alpha\beta}\left(\frac{\boldsymbol{k}_1+\boldsymbol{k}_2}{2}\right) \equiv \int \frac{d(\boldsymbol{k}_1-\boldsymbol{k}_2)}{(2\pi)^3}\Sigma_{\alpha\beta}(\boldsymbol{k}_1,\boldsymbol{k}_2,0), \tag{A1}$$

$$\phi_{\alpha\beta}\left(\frac{\boldsymbol{k}_1+\boldsymbol{k}_2}{2}\right) \equiv \int \frac{d(\boldsymbol{k}_1-\boldsymbol{k}_2)}{(2\pi)^3}\Phi_{\alpha\beta}(\boldsymbol{k}_1,\boldsymbol{k}_2,0). \tag{A2}$$

In these definitions $\boldsymbol{r}_0$ disappears. The reason is that for objects which are time independent the Eulerian and BL representations are equivalent and the designation $\boldsymbol{r}_0$ is unneeded. Here we have objects with $\omega = 0$, or time-integrated quantities. It was shown in Ref. [26] that time integrated quantities are related to simultaneous correlations, and as such they lose the $\boldsymbol{r}_0$ designation.

Denote the rest of the mass operators as

$$\tilde{\Sigma}_{\alpha\beta}(\boldsymbol{r}_0|\boldsymbol{k}_1,\boldsymbol{k}_2,\omega) \equiv \Sigma_{\alpha\beta}(\boldsymbol{r}_0|\boldsymbol{k}_1,\boldsymbol{k}_2,\omega)\sigma_{\alpha\beta}\left(\frac{\boldsymbol{k}_1+\boldsymbol{k}_2}{2}\right),$$

$$\tilde{\Phi}_{\alpha\beta}(\boldsymbol{r}_0|\boldsymbol{k}_1,\boldsymbol{k}_2,\omega) \equiv \Phi_{\alpha\beta}(\boldsymbol{r}_0|\boldsymbol{k}_1,\boldsymbol{k}_2,\omega) - \phi_{\alpha\beta}\left(\frac{\boldsymbol{k}_1+\boldsymbol{k}_2}{2}\right).$$

For translationally invariant tensors in homogeneous and incompressible turbulence one can write

$$\sigma_{\alpha\beta}(\boldsymbol{k}) = P_{\alpha\beta}(\boldsymbol{k})\sigma(k), \tag{A3}$$

$$\phi_{\alpha\beta}(\boldsymbol{k}) = P_{\alpha\beta}(\boldsymbol{k})\phi(k),$$

where $P_{\alpha\beta}(\boldsymbol{k})$ is the transverse projector

$$P_{\alpha\beta}(\boldsymbol{k}) = \delta_{\alpha\beta} - \frac{k_\alpha k_\beta}{k^2}. \tag{A4}$$

It is known [20] that $\sigma(k)$ (which is the mass operator taken at $\omega = 0$) is purely imaginary

$$\sigma(k) = -i\gamma(k), \tag{A5}$$

with $\gamma(k)$ real positive. On the other hand $\phi(k)$ is purely real. The diagrammatic series expansion of both $\gamma(k)$ and $\phi(k)$ converge order-by-order, and using scaling relations as shown in Eq. (16) one can find their scaling behavior. The order-by-order theory dictates a K41 evaluation of these objects which is

$$\gamma(k) = c_\gamma[\overline{\epsilon}k]^{2/3}, \tag{A6}$$

$$\phi(k) = c_\phi \overline{\epsilon} k^{-3}, \tag{A7}$$

where c_γ and c_ϕ are dimensionless constants.

The Dyson-Wyld equations can be written shortly as

$$(\omega + i\nu k^2)\boldsymbol{G} = \boldsymbol{P} + \boldsymbol{\Sigma}^*\boldsymbol{G}, \tag{A8}$$

$$\boldsymbol{F} = \boldsymbol{G}^*(\boldsymbol{\Phi} + \boldsymbol{D})^*\boldsymbol{G}, \tag{A9}$$

where ν is the molecular viscosity, $\boldsymbol{P}$ is the transverse projector, and $\boldsymbol{D}$ is the correlation function of the external force which is localized in the energy containing interval. The asterisk stands for summation over tensor indices and integration over intermediate $\boldsymbol{k}$. Substituting $\boldsymbol{\Sigma}$ from Eq. (A3) into the Dyson equation we rewrite

$$[\omega + i\nu k^2 + i\gamma(k)]\boldsymbol{G} = \boldsymbol{P} + \tilde{\boldsymbol{\Sigma}}^*\boldsymbol{G}. \tag{A10}$$

In the bulk of the inertial interval we can neglect νk^2 with impunity. The zero order solution of this equation is obtained by neglecting $\tilde{\boldsymbol{\Sigma}}$:

$$G_{1,1}^{\alpha\beta} \to G_{1,1}^{\alpha\beta}(\boldsymbol{k},\omega) = P_{\alpha\beta}(\boldsymbol{k})g(k,\omega), \tag{A11}$$

$$g(k,\omega) = \frac{1}{\omega + i\gamma(k)}. \tag{A12}$$

The zero order solution of $\boldsymbol{F}$ is obtained in three steps: first replace $\boldsymbol{\Phi}$ by $\boldsymbol{\phi}$, secondly neglect $\boldsymbol{D}$ in the inertial interval in comparison with $\boldsymbol{\phi}$, and finally substitute $\boldsymbol{g}$ instead of $\boldsymbol{G}$ in Eq. (A9). The result is

$$F_2^{\alpha\beta} \rightarrow F_2^{\alpha\beta}(\boldsymbol{k},\omega) = P_{\alpha\beta}(\boldsymbol{k}) f(k,\omega), \tag{A13}$$

$$f(k,\omega) = \frac{\phi(k)}{\omega^2 + \gamma^2(k)}. \tag{A14}$$

Iterating Eqs. (A8), (A9) without the bare forcing and viscosity results in a diagrammatic series which topologically is exactly the same as the old Wyld diagrammatic expansion before line resummation. The difference is twofold. First, instead of bare propagators we have K41 propagators $\boldsymbol{g}$ and $\boldsymbol{f}$, and every one-particle reducible fragment of any diagram will have a counterterm which subtracts its ''diagonal'' part. This counter term is of no consequence for our procedure here since the diagrams involving it can be resummed in the four-point vertices (the rungs) together with all the other contributions as explained in the text. The resulting topological structure of the ladder diagrams is thus unchanged in the formulation.

APPENDIX B: SELF-CONSISTENCY AT THE LEVEL OF K41

Before establishing this self-consistency we need to pass from correlation functions in $\boldsymbol{k},\omega$ representation to structure functions. The theory is done naturally in $\boldsymbol{k},\omega$ representation but the experimental scaling exponents are measured in simultaneous structure functions. We first transform from ω representation of pth-order correlation function $\boldsymbol{\mathcal{F}}_p(\{\boldsymbol{k}_j,\omega_j\})$ to simultaneous correlation function $\boldsymbol{F}_p(\{\boldsymbol{k}_j\})$ by the integration

$$\boldsymbol{F}_p(\{\boldsymbol{k}_j\}) = \int_{-\infty}^{\infty} \prod_{i=1}^{p} \frac{d\omega_i}{2\pi} \delta(\omega_1 + \cdots \omega_p) \boldsymbol{\mathcal{F}}_p(\{\boldsymbol{k}_j,\omega_j\}). \tag{B1}$$

Here $\{\boldsymbol{k}_j,\omega_j\}$ and $\{\boldsymbol{k}_j\}$ are sets of corresponding variables with $j=1,\ldots,p$. The transformation from $\boldsymbol{k}$ representation of $\boldsymbol{F}_p(\{\boldsymbol{k}_j\})$ to the pth-order structure function is done as follows: define the longitudinal component of the velocity as

$$S_p(r) = \left\langle \left\{ \left[\boldsymbol{u}\left(\frac{\boldsymbol{r}}{2}\right) - \boldsymbol{u}\left(-\frac{\boldsymbol{r}}{2}\right) \right] \frac{\boldsymbol{r}}{r} \right\}^p \right\rangle. \tag{B2}$$

Each of the factors is Fourier transformed according to

$$\left[\boldsymbol{u}\left(\frac{\boldsymbol{r}}{2}\right) - \boldsymbol{u}\left(-\frac{\boldsymbol{r}}{2}\right) \right] = \int \frac{d\boldsymbol{k}_j}{(2\pi)^3} \hat{\boldsymbol{u}}(\boldsymbol{k}_j) \left[\exp\left(i \frac{\boldsymbol{k}_j \cdot \boldsymbol{r}}{2} \right) - \exp\left(-i \frac{\boldsymbol{k}_j \cdot \boldsymbol{r}}{2} \right) \right]. \tag{B3}$$

Accordingly,

$$S_p(r) = (2\pi)^3 \int_{-\infty}^{\infty} \prod_{i=1}^{p} \frac{d\boldsymbol{k}_i}{(2\pi)^3} \delta(\boldsymbol{k}_1 + \cdots \boldsymbol{k}_p) \tag{B4}$$

$$\times f_p(\boldsymbol{r},\{\boldsymbol{k}_j\}) F_p(\{\boldsymbol{k}_j\}). \tag{B5}$$

Here

$$(2\pi)^3 F_p(\{\boldsymbol{k}_j\}) \delta(\boldsymbol{k}_1 + \cdots \boldsymbol{k}_p) = \left\langle \prod_{j=1}^{p} \hat{\boldsymbol{u}}(\boldsymbol{k}_j) \frac{\boldsymbol{r}}{r} \right\rangle. \tag{B6}$$

The functions $f_p(\boldsymbol{r},\{\boldsymbol{k}_j\})$ are seen from Eq. (B4) to be

$$f_p(\boldsymbol{r},\{\boldsymbol{k}_j\}) = \prod_{j=1}^{p} [2i \sin(\tfrac{1}{2}\boldsymbol{k}_j \cdot \boldsymbol{r})]. \tag{B7}$$

In the limit $\boldsymbol{r} \rightarrow 0$

$$f_p(\boldsymbol{r},\{\boldsymbol{k}_j\}) \propto \prod_{j=1}^{p} (\boldsymbol{k}_j \cdot \boldsymbol{r}). \tag{B8}$$

The K41 scaling exponents y_p associated with pth-order correlation function $\boldsymbol{\mathcal{F}}_p(\{\boldsymbol{k}_j,\omega_j\}) \propto k^{-y_p}$ in $(\boldsymbol{k},\omega)$ representation is

$$y_p = 4p - 11/3. \tag{B9}$$

This corresponds to $\boldsymbol{S}_p(\boldsymbol{r}) \propto r^{p/3}$ under the condition of convergence of integrals (B1), (B5).

Next consider the third-order Green's function, $G_{3,3}(\{k_j,\kappa_j\})$ in which we denoted by k_j the set of incoming wave vectors and by κ_j the set of outgoing wave vectors. The skeleton diagram of $G^{s}_{3,3}(\{k_j,\kappa_j\})$ which involves four-point rungs is shown as diagram (3) in Fig. 4(a). (The contribution of six-point rungs to the skeleton is considered in Appendix F and shown not to change the present considerations.) This skeleton has two rungs, and we consider it in the limit that the incoming k_j vectors are much larger than the outgoing κ_j. In this limit we have four Green's functions with large k, contributing γ_k^{-4}, and one vertex with all k large, contributing k. The two rungs have large k vector in them [k_5 in Eq. (22)], giving k^6. Finally, one of the rungs has large k coming and going, and Eq. (22) requires for it a $k^{2/3}$. Altogether this gives $G_{3,3}(\{k_j,\kappa_j\}) \propto k^{x_3}$ with $x_3 = 25/3$ which is equal to y_3 given by Eq. (B9). This means that the skeleton diagrams for $G_{3,3}(\{k_j,\kappa_j\})$ (with asymptotics of the rung defined by the two-point fusion rules) automatically reproduces the K41 scaling exponent $\zeta_3 = 1$ in the three-point fusion. This is true subject to the condition that the integrals (B1), (B5) for $p=3$ converge. That this is so may be shown by a direct calculation. For future purposes it is extremely important to note that the principal contribution to the $\boldsymbol{k}$ integral (B5) comes from the region where $k_1 \sim k_2 \sim k_3 \sim 1/r$.

Now let us compare diagram (3) in Fig. 4(a) and Fig. 5 with the skeleton diagrams for $G_{3,3}$ and $G_{4,4}$. One recognizes that in general for $G_{p,p}$, we will have $(p-1)$ rungs with large incoming k, contributing $k^{-3(p-1)}$ [originating from k_e in Eq. (22)]. We will have also $2p-2$ Green's functions with large k contributing $k^{-(2p-2)2/3}$. Next we will have $p-2$ outgoing legs with large k contributing $k^{-(p-2)2/3}$

from Eq. (9). Finally we will have $2p-2$ vertices having incoming and outgoing large k vectors, contributing k^{p-2}. All together we find that $G_{p,p}(\{k_j,\kappa_j\}) \propto k^{-x_p}$ with $x_p=4p-11/3$ which is equal to y_p given by Eq. (B9). Convergence of the $\boldsymbol{k}$ integral (B5) for $p=4$ may be shown by direct calculations. A proof of convergence of the $\boldsymbol{k}$ integrals (B5) for $p>4$ is a tedious exercise which nevertheless may be done, for example, iteratively. It is readily demonstrated that the integral converges when all k_j vectors are of the same order of magnitude (say, k). Then $G_{p,p} \sim k^{11/3-4p}$. After $(p-1)$ ω integrations (each of them giving a factor $k^{2/3}$) one has $k^{3(p-1)-p/3}$ which is enough for convergence of $(p-1)$ d^3k integrals in the UV region $k_j \sim k \gg 1/r$. In the IR region $k_j \sim k \ll 1/r$ the functions f_p provide the integral with additional k^p factor [according to Eq. (B8)] which guarantees the convergence.

The considerations of the six-point and higher-order rungs leave these conclusions invariant.

APPENDIX C: ANALYSIS OF TWO-LOOP INTEGRALS CONTRIBUTING TO ζ_2

The integrand in the integral (66) is a function of q_1 and q_2 and it depends on k and κ as parameters. The integration range is the q_1-q_2 infinite plane, but in the limit $k \gg \kappa$ the main contribution comes from the four finite quadrants $\kappa < |q_1|,|q_2| < k$. Well inside the quadrants we are allowed to use the asymptotic form in which $\kappa \ll |q_1|,|q_2| \ll k$. In this regime the integrand is k,κ independent, and the dependence of the integrals on k,κ appears only via the limits of integration. By changing the dummy variables q_1 and q_2 we can now project all four quadrants into one of them, say q_1 and q_2 positive. In this asymptotic regime we can use for the rungs in the integrand of Eq. (66) that include either k or κ their asymptotic form (32). This results in

$$K(k,\kappa)=\tilde{\delta}^2\int_p^k \frac{dq_1}{q_1}\int_p^k \frac{dq_2}{q_2}\Psi(q_1,q_2), \tag{C1}$$

$$\Psi(q_1,q_2)=\tilde{\Psi}(q_1,q_2)-\tilde{\Psi}(-q_1,q_2). \tag{C2}$$

In Appendix D we show how to analyze this kind of integral with the aim of extracting the coefficients of the leading and first subleading logarithmic terms, i.e.,

$$K_1(k,\kappa)=\frac{a_1}{2}\ln^2(k/\kappa)+b_1\ln(k/\kappa). \tag{C3}$$

Using the results there (D4) with $\tilde{\Psi}(q_1,q_2)=\tilde{\Psi}_1(q_1,q_2)$,

$$\tilde{\Psi}_1(q_1,q_2)=\frac{q_1^3|q_1-q_2|\mathrm{sgn}(q_2)}{2(q_1^2-q_1q_2+q_2^2)^2}, \tag{C4}$$

one find immediately $a \to a_1=1$ as required by the anticipated expansion employed in Eqs. (44)–(46). To compute b_1 we examine the integral $b_1(A)$ numerically, see Fig. 6. We see that the requested limit exists and that $b_1 \approx -0.434$.

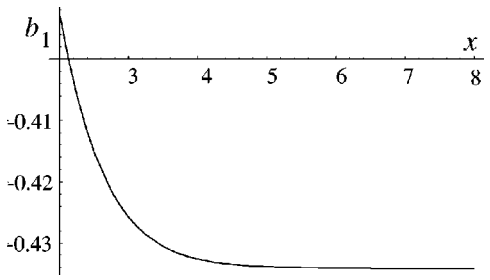

FIG. 6. Numerically computed dependence of $b_1(A)$ with $A=\exp(x)$.

APPENDIX D: EXTRACTION OF THE SUBLEADING LOGARITHMIC TERM FROM THE TWO-LOOP INTEGRALS

The two-loop integrals have the characteristic structure appearing in Eq. (C1)

$$I(A)=\tilde{\delta}^2\int_1^A \frac{dq_1}{q_1}\int_1^A \frac{dq_2}{q_2}\Psi(q_1,q_2), \tag{D1}$$

where $A \gg 1$ and $\Psi(q_1,q_2)$ are homogeneous functions of degree zero: $\Psi(\lambda q_1,\lambda q_2)=\Psi(q_1,q_2)$. When $\Psi(q_1,q_2)=1$ then $I(A)=\ln^2 A$. In general only the leading term of $I(A)$ is proportional to $\ln^2 A$ and we expect the following subleading terms:

$$I(A)=\tilde{\delta}^2\left[\frac{a}{2}\ln^2 A+b\ln A+c+\frac{d}{A}+\cdots\right]. \tag{D2}$$

Our goal is to find the coefficient b in the limit $A \to \infty$. Taking the first derivative of Eq. (D2) with respect to A and multiplying by A we find

$$a\ln A+b-\frac{d}{A}-\cdots=\int_1^A \frac{dq_2}{q_2}\Psi(1,q_2)+\int_1^A \frac{dq_1}{q_1}\Psi(q_1,1)$$
$$=\int_{1/A}^1 \frac{dx}{x}\Psi(x,1)+\int_{1/A}^1 \frac{dy}{y}\Psi(1,y), \tag{D3}$$

where we changed the dummy variables $q_1=xA$ and $q_2=yA$. Taking another derivative and multiplying by A we find for large A

$$a=\Psi\left(1,\frac{1}{A}\right)+\Psi\left(\frac{1}{A},1\right). \tag{D4}$$

Substituting this result in Eq. (D3), and representing $\ln A$ as $\int_{1/A}^1 dx/x$ we find

$$b=\lim_{A\to\infty} b(A), \tag{D5}$$

$$b(A)=\int_{1/A}^1 \frac{dx}{x}\left[\Psi(x,1)+\Psi(1,x)-\Psi\left(\frac{1}{A},1\right)-\Psi\left(1,\frac{1}{A}\right)\right].$$

If the expansion assumed in Eq. (D2) is valid, this limit must exist.

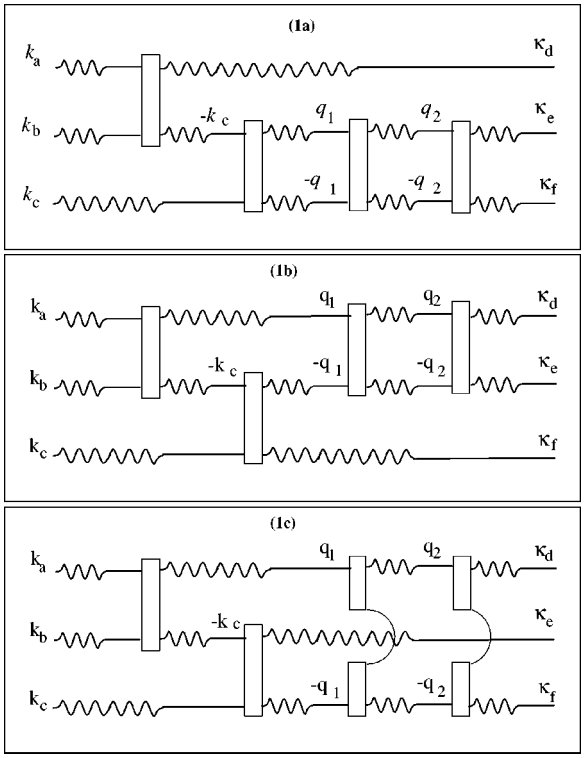

FIG. 7. The first group of three two-loop diagrams appearing in the loop expansion of $G_{3,3}$.

APPENDIX E: THE NINE TWO-LOOP DIAGRAMS OF $G_{3,3}$

Consider diagram (1a) in Fig. 7. We are interested in the ratio of $T^{(2)}_{3,1a}/T^{s}_{3}$, where $T^{(2)}_{3,1a}$ is obtained by substituting the diagram (1a) instead of $G_{3,3}$ in Eq. (49). In the asymptotic regime $\kappa r \ll 1$ the loop integrals over q_1 and q_2 contribute mostly in the regime $k \gg q_1, q_2 \gg \kappa$. In this regime the integrals over $k_a, \omega_a, k_b, \omega_b$ cancel in the desired ratio. Similarly the Green's functions $G(\kappa_d)$, $G(\kappa_e)$, and $G(\kappa_f)$ also cancel in the ratio. Accordingly $T^{(2)}_{3,1a}/T^{s}_{3}$ can be calculated from the *amputated* diagram (2) in Fig. 9, in which the explicit dependence on k_j and κ_j has disappeared. These wave vectors remain only in the limits of the integrals over q_1 and q_2, with k replaced by $1/r$. In this diagram every black dot contributes a factor of $q_j^{1/3+\delta_a}$ where q_j is the wave vector on the right of the black dot. This is a remnant of the corresponding rung before the amputation. The thin line connecting these dots is just a reminder that we have loop integrals to perform.

The point to understand now is that if we use diagrams (1b) and (1c) in Fig. 7 to form $T^{(2)}_{3,1b}$ and $T^{(2)}_{3,1c}$, the ratio of these to T^{s}_{3} can be again calculated from the amputation of their own diagrams. This will lead to the *identical* amputated diagram (2) of Fig. 9. In addition, and most importantly, the integral that needs to be computed is the same as Eq. (66). Thus one recaptures Eq. (67) but with the combinatorial factor 3 in front of the RHS:

$$T^{(2)}_{3,1a+1b+1c}(r,\kappa) = 3\tilde{\delta}^2\left[\frac{1}{2}\ln^2\left(\frac{1}{\kappa r}\right) + b_1 \ln\left(\frac{1}{\kappa r}\right)\right] T^{s}_{3}(r,\kappa), \tag{E1}$$

with b_1 of Eq. (68).

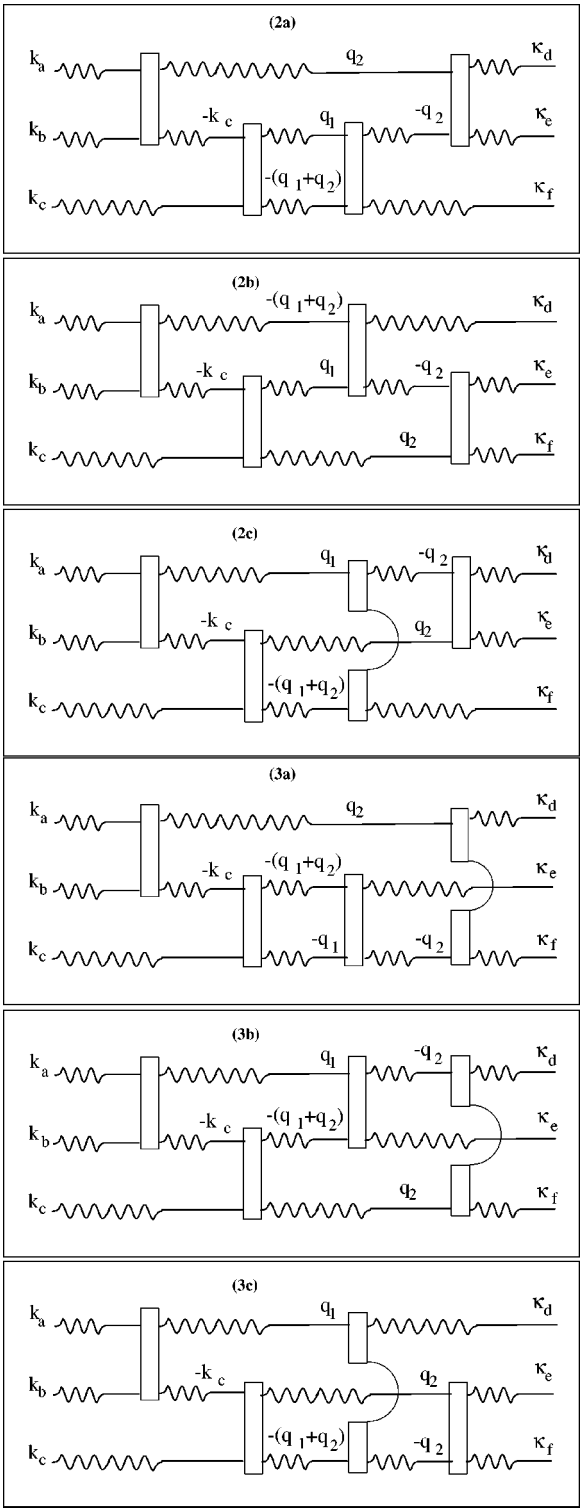

FIG. 8. The second group of six two-loop diagrams appearing in the loop expansion of $G_{3,3}$.

The second group of six diagrams [(2a)–(3c)] shown in Fig. 8 yields a similar analysis, but the amputated diagram is shown as diagram (3) in Fig. 9. All six diagrams result in the very same amputation, up to permutations of the three struts. Analyzing the amputated diagram (3) one brings it to the canonical form (C1) with $\tilde{\Psi}(q_1, q-2)$ given by Eq. (70). Accordingly we write

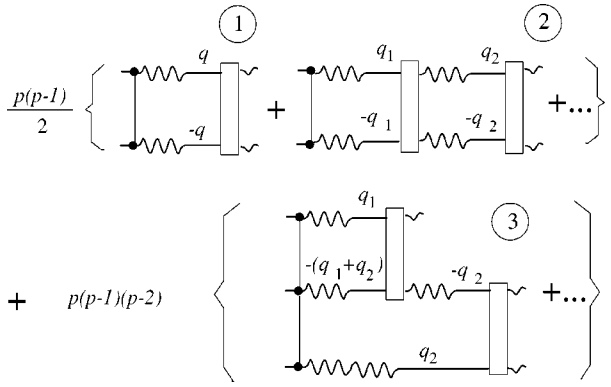

FIG. 9. The amputated diagrams that appear up to two-loop in the loop expansion of $G_{p,p}$, with the appropriate combinatorial factors.

$$T^{(2)}_{3,2a,\ldots,3c}(r,\kappa)=6\tilde{\delta}^2\left[\frac{1}{2}\ln^2\left(\frac{1}{\kappa r}\right)+b_2\ln\left(\frac{1}{\kappa r}\right)\right]T^s_3(r,\kappa), \tag{E2}$$

with b_2 of Eq. (71).

The analysis of the two-loop diagrams that involve four-point rungs in the context of $G_{p,p}$ follows exactly the same lines, with the amputated diagrams being those of Fig. 9. The only thing to mind is the combinatorics, which are presented explicitly in Fig. 9, leading to the numbers in Eq. (75).

APPENDIX F: RESUMMED EQUATIONS FOR THE FOUR-POINT AND SIX-POINT RUNGS

In this appendix we sketch a theory for the four-point and six-point rungs. Our main aim here is to explain why the six-point rung is quadratic in the smallness, but we use the opportunity to indicate how a future theory of these objects may be formulated.

Consider the beginning of the series expansion of the four-point rung which is shown in Fig. 2(b). Diagram (2) contains a cross of correlators each attached to two three-point vertices. This is exactly diagram (1), and therefore the equation can lend itself to resummation resulting in the equation shown in Fig. 10(a). We note that this is not the full equation for the four-point rung even in one-loop order since we did not take into account the ladders with a correlator and Green's function in a cross section. Taking into account all the needed contributions is not difficult, but is not the main point of this appendix, and we proceed for simplicity without the additional terms.

In the asymptotic regime the bare contribution diagram (1) in Fig. 10(a) is negligible. With this contribution discarded, the remaining equation is homogeneous, calling for finding a zero mode of the equation. Since we have already demonstrated that the four-point rung is small, of the order of δ_2 we can conclude that the loop integral which we denote as l_1 must be large, or the order of $1/\delta_2$ (the homogeneous equation can be only solved if $\delta_2\approx\delta_2^2 l_1$). In fact, in the future it would be extremely worthwhile to solve the full equation in one-loop order and demonstrate that this is the case, and thus to lend further weight to the theory presented in this paper. Of course solving such an equation will also

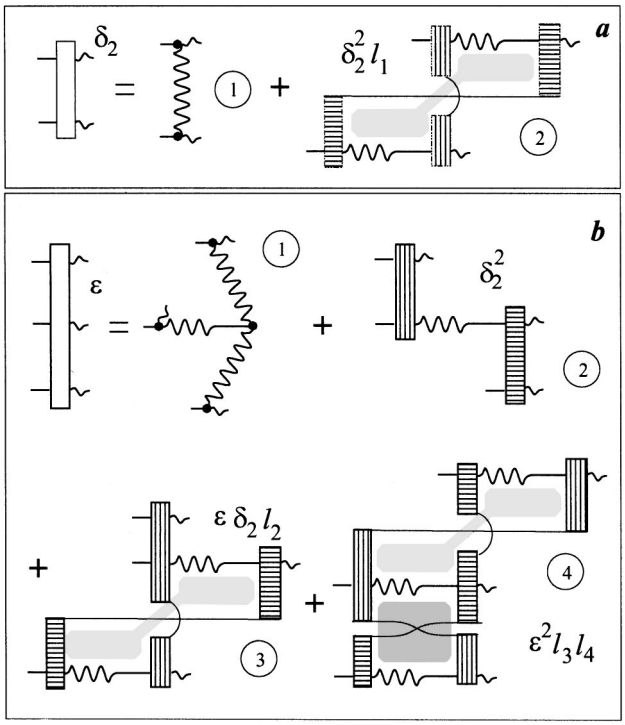

FIG. 10. A sketch of the equations for the four-point rung (a) and six-point rung (b). The shading of rungs is used to identify different pieces of the same object. In the same manner we shade the loops to identify one or two loop integrals.

supply us with a functional form of the four-point rung, and with it a substantial part of the value of the parameter b_2 which appears in the final result for the scaling exponents.

In Fig. 10(b) we present the resummed form of the equation of the six-point rung, to the same level of qualitative discussion. Again we discard in the asymptotic limit the bare contribution of diagram (1), but we cannot neglect diagram (2) since it has the same asymptotic behavior as the resummed six-point rung. Diagram (2) is of the order of δ_2^2. Diagram (3) is of the order of $\epsilon\delta_2 l_2$ where l_2 is the loop integral. This integral is very similar to l_1, and we therefore estimate $l_2\approx l_1\approx 1/\delta_2$, and thus diagram (3) is of the order of the left-hand side. Diagram (4) is of the order of $\epsilon^2 l_3 l_4$, where l_3 and l_4 each refer to one of the loop integrals. With the same level of approximation we estimate it thus to be of $O(\epsilon^2/\delta_2^2)$. Denoting $x\equiv\epsilon/\delta^2$ we thus represent the order of magnitude relations that result from panel (b) by the equation

$$x=1+ax+bx^2, \tag{F1}$$

where a and b are dimensionless constants of $O(1)$. It is obvious that only $x\approx 1$ is a consistent solution of this equation, and we thus conclude that the six-point rung is quadratic in the smallness δ_2.

We therefore understand that the six-point rung appears in our considerations only at the level of the $O(\delta^2)$ order. In this order it appears in addition to the two-loop integrals which are formed by two four-point rungs, as discussed in detail in the text of the paper. But since the six-point rung connects three struts, exactly as the structure made of *two*

four-point rungs, the combinatorical factors appearing in the pth order scaling exponents *are identical*. Accordingly we understand that the effect of the six-point rung is only in renormalizing the value of the parameter b_2 which is model dependent anyway.

A similar consideration applies to the eight-point rung which begins to affect the theory only in $O(\delta_2^3)$. It will renormalize the value of the parameter b_3 in Eq. (78). Higher-order rungs are even less relevant for the calculation at hand.

[1] A. N. Kolmogorov, Dokl. Akad. Nauk SSSR **30**, 9 (1941).
[2] A. S. Monin and A. M. Yaglom, *Statistical Fluid Mechanics: Mechanics of Turbulence* (MIT Press, Cambridge, MA, 1973), Vol. II.
[3] F. Anselmet, Y. Gagne, E. J. Hopfinger, and R. A. Antonia, J. Fluid Mech. **140**, 63 (1984).
[4] K. R. Sreenivasan and P. Kailasnath, Phys. Fluids A **5**, 512 (1993).
[5] R. Benzi, S. Ciliberto, R. Tripiccione, C. Baudet, F. Massaioli, and S. Succi, Phys. Rev. E **48**, R29 (1993).
[6] R. Benzi, S. Ciliberto, C. Baudet, and G. Ruiz-Chavarria, Physica D **80**, 385 (1995).
[7] Uriel Frisch, *Turbulence: The Legacy of A. N. Kolmogorov* (Cambridge University Press, Cambridge, 1995).
[8] A. N. Kolmogorov, J. Fluid Mech. **13**, 82 (1962).
[9] R. H. Kraichnan, Phys. Fluids **11**, 945 (1968).
[10] R. H. Kraichnan, Phys. Rev. Lett. **72**, 1016 (1994).
[11] K. Gawedzki and A. Kupiainen, Phys. Rev. Lett. **75**, 3608 (1995).
[12] I. Arad, V. S. L'vov, E. Podivilov, and I. Procaccia, Phys. Rev. E (to be published); e-print chao-dyn/9907017.
[13] L. Ts. Adzhemyan, N. V. Antonov, and A. V. Vasil'ev, Phys. Rev. E **58**, 1823 (1998).
[14] Y. Cohen, V. S. L'vov, A. Pomyalov, and I. Procaccia (unpublished).
[15] V. I. Belinicher, V. S. L'vov, A. Pomyalov, and I. Procaccia, J. Stat. Phys. **93**, 797 (1998).
[16] V. S. L'vov and I. Procaccia, Phys. Rev. E **52**, 3858 (1995).
[17] V. S. L'vov and I. Procaccia, Phys. Rev. Lett. **76**, 2896 (1996).
[18] V. S. L'vov and I. Procaccia, Phys. Rev. E **53**, 3468 (1996).
[19] V. S. L'vov and I. Procaccia, Phys. Rev. E **52**, 3840 (1995).
[20] H. W. Wyld, Ann. Phys. (N.Y.) **14**, 143 (1961).
[21] P. C. Martin, E. D. Siggia, H. A. Rose, Phys. Rev. A **8**, 423 (1973).
[22] V. S. L'vov and I. Procaccia, in *Fluctuating Geometries in Statistical Mechanics and Field Theory*, edited by F. David P. Ginsparg, and J. Zinn-Justin, Les Houches session LXII, 1994 (Elsevier, Amsterdam, 1995).
[23] V. I. Belinicher and V. S. L'vov, Zh. Éksp. Teor. Fiz. **93**, 1269 (1987) [Sov. Phys. JETP **66**, 303 (1987)].
[24] R. H. Kraichnan, J. Fluid Mech. **83**, 349 (1977).
[25] A. L. Fairhall, O. Gat, V. S. L'vov, and I. Procaccia, Phys. Rev. E **53**, 3518 (1996).
[26] V. S. L'vov, E. Podivilov, and I. Procaccia, Phys. Rev. E **55**, 7030 (1997).
[27] V. S. L'vov and V. Lebedev, Phys. Rev. E **47**, 1794 (1993).